Clinica Chimica Acta 406 (2009) 179–180

Contents lists available at ScienceDirect

Clinica Chimica Acta

journal homepage: www.elsevier.com/locate/clinchim

Letter to the Editor

Effects of the time intervals between venipuncture and serum preparation for serum peptidome analysis by matrix-assisted laser desorption/ionization time-of-flight mass spectrometry

Dear Editor:

With the recent advances in proteomics technologies, protein and peptide biomarker discovery is now one of the major applications of proteome research [1,2]. Profiling methods based on mass spectrometry (MS) such as surface enhanced laser desorption/ionization time-of-flight (SELDI-TOF) MS and matrix-assisted laser desorption ionization time-of-flight (MALDI-TOF) MS analysis of blood samples are promising tools for biomarker discovery [3,4].

However, several studies indicated that preanalytical factors have significant effects on the results of blood proteome analysis [5–13]. Appropriate specimen collection and handling towards the standardization of parameters for plasma proteome samples has been established by the HUPO plasma proteome project [14]. On the other hand, appropriate conditions for serum sample processing for peptidome analysis has not yet been fully established.

Among various preanalytical factors tested so far, the time intervals between venipuncture and serum separation (clotting time) could have significant effects on the results [11–13]. We determined in detail the effects of the clotting time on the profiles of serum peptidome analyses. Other preanalytical factors related to clinical laboratory such as freezing methods and the effects of freeze–thaw cycles were also assessed.

α-Cyano-4-hydroxycinnamic acid (CHCA) matrix (Bruker Daltonics, Bremen, Germany) solution was diluted as 0.3 g/l in ethanol:acetone (2:1) solution. Acetone and ethanol were HPLC-grade and were from Wako Pure Chemical Industries (Osaka, Japan). We collected serum samples from a total of 7 healthy volunteers (5 males, 2 females, 29–47 y) with written informed consent. The sample collection, handling and storage conditions were defined according to the specific experimental conditions as described in the text. Otherwise, serum samples were collected as follows; blood samples were collected in vacutainer tubes (InsepakII, Sekisui Kagaku Kogyo, Tokyo, Japan). After collection, the samples were allowed to clot at room temperature for 1 h and then sera were separated by centrifugation at 1500 ×g for 10 min at 4 °C. Sera were divided into aliquots in SUMILON Proteosave® SS 1.5 ml tube (Sumitomo Bakelite, Tokyo, Japan) and were stored at −80 °C until analysis.

Serum sampling and handling procedures for the analysis of each preanalytical factor were as follows. Except for the experiments to test the effects of various clotting time for serum protein profiles, serum samples were obtained by centrifugation 1 h after venipuncture. 1) For the assessment of the effects of clotting time, sera were collected 15 min, 30 min, 1, 2, 4, and 6 h after venipuncture in 4 subjects. 2) For the assessment of the effects of freezing methods, serum samples obtained from 3 subjects were frozen with liquid nitrogen or directly in freezers (−80 or −20 °C). The frozen samples were thawed on ice after one week and were subjected to analyses. 3) For the assessment of the effects of freeze/thaw cycles, 3serum samples were frozen directly in the −80 °C deep freezer and were then thawed on ice. One to seven freeze/thaw cycles were performed.

We employed magnetic beads with C8-hydrophobic interaction chromatography (C8), weak cation exchange (WCX) or immobilized metal affinity chromatography (IMAC-Cu) resin and performed serum peptidome fractionation with these 3 magnetic beads according to the manufacturer's protocol. A portion of the eluted sample (1 μl) was mixed with 10 μl of CHCA matrix. Then, 0.8 μl of the resulting mixture was spotted onto AnchorChip™ target plate, and crystallized. Every samples were duplicated, and quadricate spotting were performed for one elution. For data analysis, spectra from these eight spots were averaged. All these procedures were performed automatically with ClinProtRobot (Bruker Daltonics).

The AnchorChip™ target plate was placed in an AutoflexII TOF/TOF MS (Bruker Daltonics) controlled by Flexcontrol™2.4 software (Bruker Daltonics). The instrument is equipped with a 337 nm nitrogen laser, delayed-extraction electronics, and a 25 Hz digitizer. All acquisitions were generated by an automated acquisition method included in the instrument software and based on averaging 1000 randomized shots. The acquisition laser power was set between 20 and 35%. Spectra were acquired in positive linear mode, in the mass range of 600–10,000 Da. Peak clusters were completed using second pass peak section (signal to noise ratio >5). Then, we analyzed serum peptidome data with ClinProtools 2.1 software (Bruker Daltonics).

Time courses of the relative intensity of each peak appear to be categorized as 3 patterns as indicated in Fig. 1A (Types A–C). It was possible to classify all the peaks obtained into these 3 types as summarized in Fig. 1B. In analyses with WCX and C8 beads, more than half of the peaks were categorized as type C. On the other hand, type B was most common when IMAC-Cu bead were used.

3 different freezing methods, freezing in liquid nitrogen, freezing in freezer (−20 °C, −80 °C) were compared in 3 different samples. The relative intensities of each peak obtained under these 3 conditions were quite consistent when serum samples were frozen in liquid nitrogen and −80 °C freezer.

Effects of freeze/thaw cycles on serum peptide profiles were also assessed in 3 different samples. CVs of relative intensities of each peak among various freeze/thaw cycles were obtained. Numbers of peaks in which CV was >20% were few when the freeze/thaw was within 2 cycles.

Clotting time was by far the most influential preanalytical factor tested in this study. Time-dependent changes of serum proteome profiles based on magnetic bead separation and MALDI-TOF MS before centrifugation of the blood samples have been described previously [11–13]. Most previous reports, however, looked at only selected peaks in blood samples in contrast to the present study in which the effects of clotting time on all the detectable peptide peaks were evaluated. We found the effects of clotting time on time courses of the relative intensity of each peak can be categorized into 3 groups. To give an example, the 5.9 kDa peptide that we previously reported as a promising biomarker of excessive alcohol consumption [15–17] was categorized as type C, the most stable type. In the process of biomarker discovery by serum

0009-8981/$ – see front matter
doi:10.1016/j.cca.2009.06.007

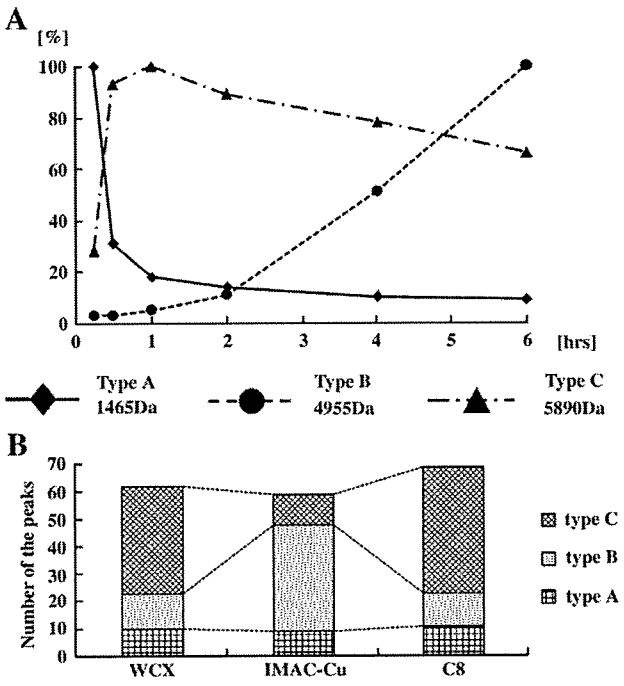

Fig. 1. Time courses of the intensities of serum peptide peaks between venipuncture and serum separation. (A) In type A, the relative intensities of the peak decrease in a time-dependent manner after venipuncture. On the other hand, the relative intensities increase in type B. In type C, they increase remarkably during the first 30 min, but are relatively stable thereafter. (B) The number of peaks categorized as types A–C.

peptidome analyses, one may have to consider the time course of the marker candidate after venipuncture and to know in which type of the patterns the particular marker can be categorized.

The number of peaks detectable by the ClinProt™ system was largest when serum samples were obtained around 60 min after venipunctures. It will be reasonable to set time intervals of 60 min between venipuncture and serum separation for efficient marker discovery by serum peptidome analyses.

The ideal way to freeze and store serum samples is to use liquid nitrogen and its container. It is not necessarily practical to use liquid nitrogen on a routine basis; some alternatives are required to conduct multi-center validation study. As long as short-term storage is concerned, our data indicated that serum proteome profiles obtained by samples frozen and stored at −80 °C were comparable to those obtained by samples frozen and stored in liquid nitrogen. Also, it was shown that freezing and thawing sample more than twice should be avoided, suggesting that serum samples for serum peptidome analyses have to be initially divided into aliquots.

Careful sample collection and handling procedures should have profound impact on serum peptidome patterns, especially in inter-laboratory or multi-center studies. The results of this study indicate that clotting time is a critical preanalytical factor, and that serum peptide peaks can be categorized into 3 groups in terms of their time courses. It is essential to know to which group each candidate peak belongs when planning and conducting validation studies.

References

[1] Righetti PG, Castagna A, Antonucci F, et al. Proteome analysis in the clinical chemistry laboratory: myth or reality? Clin Chim Acta 2005;357:123–39.
[2] Colantonio DA, Chan DW. The clinical application of proteomics. Clin Chim Acta 2005;357:151–8.
[3] Diamandis EP. Mass spectrometry as a diagnostic and a cancer biomarker discovery tool: opportunities and potential limitations. Mol Cell Proteomics 2004;3:367–78.
[4] Hortin GL. The MALDI-TOF mass spectrometric view of the plasma proteome and peptidome. Clin Chem 2006;52:1223–37.
[5] Banks RE, Stanley AJ, Cairns DA, et al. Influences of blood sample processing on low-molecular-weight proteome identified by surface-enhanced laser desorption/ionization mass spectrometry. Clin Chem 2005;51:1637–49.
[6] Albrethsen J, Bogebo R, Olsen J, Raskov H, Gammeltoft S. Preanalytical and analytical variation of surface-enhanced laser desorption-ionization time-of-flight mass spectrometry of human serum. Clin Chem Lab Med 2006;44:1243–52.
[7] Timms JF, Arslan-Low E, Gentry-Maharaj A, et al. Preanalytic influence of sample handling on SELDI-TOF serum protein profiles. Clin Chem 2007;53:645–56.
[8] West-Norager M, Kelstrup CD, Schou C, Hogdall EV, Hogdall CK, Heegaard NH. Unravelling in vitro variables of major importance for the outcome of mass spectrometry-based serum proteomics. J Chromatogr B Analyt Technol Biomed Life Sci 2007;847:30–7.
[9] Yi J, Kim C, Gelfand CA. Inhibition of intrinsic proteolytic activities moderates preanalytical variability and instability of human plasma. J Proteome Res 2007;6:1768–81.
[10] Luque-Garcia JL, Neubert TA. Sample preparation for serum/plasma profiling and biomarker identification by mass spectrometry. J Chromatogr A 2007;1153:259–76.
[11] West-Nielsen M, Hogdall EV, Marchiori E, Hogdall CK, Schou C, Heegaard NH. Sample handling for mass spectrometric proteomic investigations of human sera. Anal Chem 2005;77:5114–23.
[12] Hsieh SY, Chen RK, Pan YH, Lee HL. Systematical evaluation of the effects of sample collection procedures on low-molecular-weight serum/plasma proteome profiling. Proteomics 2006;6:3189–98.
[13] Baumann S, Ceglarek U, Fiedler GM, Lembcke J, Leichtle A, Thiery J. Standardized approach to proteome profiling of human serum based on magnetic bead separation and matrix-assisted laser desorption/ionization time-of-flight mass spectrometry. Clin Chem 2005;51:973–80.
[14] Rai AJ, Gelfand CA, Haywood BC, et al. HUPO Plasma Proteome Project specimen collection and handling: towards the standardization of parameters for plasma proteome samples. Proteomics 2005;5:3262–77.
[15] Nomura F, Tomonaga T, Sogawa K, et al. Identification of novel and downregulated biomarkers for alcoholism by surface enhanced laser desorption/ionization-mass spectrometry. Proteomics 2004;4:1187–94.
[16] Sogawa K, Itoga S, Tomonaga T, Nomura F. Diagnostic values of surface-enhanced laser desorption/ionization technology for screening of habitual drinkers. Alcohol Clin Exp Res 2007;31:S22–6.
[17] Nomura F, Tomonaga T, Sogawa K, Wu D, Ohashi T. Application of proteomic technologies to discover and identify biomarkers for excessive alcohol consumption: a review. J Chromatogr B Analyt Technol Biomed Life Sci 2007;855:35–41.

Hiroshi Umemura*
Masahiko Nezu
Mamoru Satoh
Asako Kimura
Takeshi Tomonaga
Fumio Nomura
Department of Molecular Diagnosis, Graduate School of Medicine, Chiba University, Japan
*Corresponding author. Department of Molecular Diagnosis, Graduate School of Medicine, Chiba University, 1-8-1 Inohana, Chuo-ku, Chiba City, Chiba, Japan 260-8670.
Tel.: +81 43 226 2167; fax: +81 43 226 2169.
E-mail address: UGN11252@nifty.com (H. Umemura).

Yoshio Kodera
Department of Physics, School of Science, Kitasato University, Japan

23 March 2009

[Frontiers in Bioscience 14, 3401-3408, January 1, 2009]

c-myc suppressor FBP-interacting repressor for cancer diagnosis and therapy

Kazuyuki Matsushita[1], Takeshi Tomonaga[1], Toshiko Kajiwara[1], Hideaki Shimada[5], Sakae Itoga[1], Takaki Hiwasa[3], Shuji Kubo[4], Takenori Ochiai[2], Hisahiro Matsubara[2], Fumio Nomura[1]

[1]Departments of Molecular Diagnosis & Division of Clinical Genetics and Proteomics, [2]Department of Frontier Surgery, and [3]Biochemistry and Genetics, Chiba University, Graduate School of Medicine, 1-8-1 Inohana, Chuo-ku, Chiba 260-8670 , [4]Laboratory of Host Defenses, Institute for Advanced Medical Sciences, Hyogo College of Medicine, 1-1 Mukogawa-cho, Nishinomiya-shi, Hyog, [5]Department of Gastrointestinal Surgery, Chiba Cancer Center, 666-2 Nitona, Chuo-ku Chiba-shi, Chiba

TABLE OF CONTENTS

1. ABSTRACT

Based on the genetic background of cancer, we have been trying to develop novel diagnostic and therapeutic strategies against human cancers. *c-myc* gene activation has been detected in many human cancers, indicating a key role of *c-myc* in tumor development. Thus targeting *c-myc* gene suppression is a promising strategy for cancer treatment. Recently, an interaction between FIR (FUSE-Binding Protein-Interacting Repressor) and TFIIH/p89/XPB helicase was found to repress *c-myc* transcription and so might be important for suppressing tumor formation. Previously, we have shown that the expression of splicing variant of FIR is elevated in colorectal cancer tissues and promotes tumor development by disabling FIR-repression to sustain high levels of c-Myc, opposing apoptosis in cancer cells. In this study, FIR recombinant adenovirus vector induces tumor growth suppression against tumor xenografts in animal model experiment. Together, one clue to the development of cancer diagnosis and therapies directed against c-Myc may go through FIR and its splicing variant.

2. INTRODUCTION

Surgical excision alone infrequently results in long-term survival for advanced gastrointestinal cancers, thus efforts are now focused on combined treatments in an attempt to improve local control and eliminate micro-metastasis at the time of operation (1, 2). Despite improvement of surgical treatment and chemotherapies to advanced cancers, the prognosis is poor in those tumors. Significant growth suppression was observed by infection with p53 recombinant adenoviral vector (Ad-p53) in human esophageal squamous cell carcinoma cell lines. Our group has performed a clinical trial of Ad-p53 for un-resectable advanced human esophageal cancer treatment. So far the efficiency of Ad-p53 for cancer treatment is not satisfactory, thus a novel molecular target is required.

c-Myc plays an essential role in cell proliferation and tumorigenesis. *c-myc* activation was also shown to be required for skin epidermal and pancreatic beta-cell tumor maintenance in c-MYC-ER^{TAM} transgenic mice (3). *c-myc* expression level reflects interferon-gamma production in

colorectal cancer tissues and this host's immune response was associated with the better long-term survival of colorectal cancer patients (4). These observations have encouraged us for the future development of cancer therapies targeting *c-myc*. The Far UpStream Element (FUSE) is a sequence required for proper expression of the human *c-myc* gene. The FUSE is located 1.5 kb upstream of *c-myc* promoter P1, and binds the FUSE Binding Protein (FBP), a transcription factor stimulating *c-myc* expression in a FUSE dependent manner (5, 6). Yeast two-hybrid analysis revealed that FBP binds to a protein that has transcriptional inhibitory activity termed the FBP Interacting Repressor (FIR), and FIR was found to engage the TFIIH/p89/XPB helicase and repress *c-myc* transcription by delaying promoter escape (7).

Up to 60% of all human genes present at least one alternative splice variant (8). Alternative splicing has been documented to play a significant role in human disease including cancer (9). We have previously reported that a splice variant of the *c-myc* repressor FIR plays an important role in the pathogenesis of human colorectal cancer (10). A splicing variant of FIR that lacks exon2 (FIRdel/exon2), expresses mainly in tumor tissues, but not in the adjacent normal tissue. FIRdel/exon2 failed to repress c-Myc and inhibited FIR-induced apoptosis suggesting an important role for this splicing variant of FIR in the tumorigenesis of human colorectal cancer (10). In this study, enforced FIR expression by adenovirus vector in tumors for cancer therapy and detection of FIR and/or FIRdel/exon2 in the peripheral blood for cancer diagnosis are discussed.

3. MATERIALS AND METHODS

3.1. Plasmids

Full-length FIR cDNA (HA-FIR) and the FIR deleted of its first seventy-seven amino acids (HA-FIRdel/N77), and the alternatively spliced form of FIR lacking exon 2 (HA-FIRdel/exon2), obtained from cancer tissues, were cloned into the pCGNM2 vector plasmid (10), respectively, to introduce the hemagglutinin (HA)-tag at their amino termini. The human c-Myc expression vector, pcDNA3.1-*c-myc*, GeneStorm® Expression-Ready Clones (Invitrogen Co., AL) was purchased and c-Myc expression was confirmed by western blot using anti-c-Myc (Upstate Biotechnology, NY). Full-length FIR cDNA was cloned into pcDNA3.1 to generate pcDNA3.1-FIR.

3.2. Human tissue samples

Tissues from 15 cases of primary colorectal cancer were surgically excised. Written informed consent was obtained from each patient prior to surgery. The tumor samples were obtained from tumor epithelium immediately after operative excision tissues and the corresponding non-tumor epithelial samples were 5-10 cm from the tumor. All excised tissues were immediately placed into liquid nitrogen and stored at –80°C until analysis.

3.3. Immunocytochemistry

HeLa cells were grown on coverslips overnight and then transfected with plasmids using Lipofectamine Plus reagents (Invitrogen, Carlsbad, CA). At the indicated time after plasmid transfection, cells were treated for immunocytochemistry as previously described (10). The primary antibodies, mouse monoclonal anti-HA (Santa Cruz Biotechnology, CA), rabbit polyclonal anti-c-Myc (Upstate Biotechnology, NY), were diluted 1:500 and 1:200 in the blocking buffer, respectively. The primary rabbit polyclonal antibody against FIR was prepared using two synthetic peptides GDKWKPPQGTDSIKME and EVYDQERFDNSDLSA simultaneously immunized to enhance the possibility of antibody production (JAPAN BIO SERVICES Co Ltd, Saitama, Japan), and was diluted 1:200 in the blocking buffer. The coverslips were incubated at room temperature for 1 hr. After washing with PBS, the secondary antibodies, Alexa Fluor™ 488-conjugated goat anti-rabbit or 594-conjugated goat anti-mouse IgG secondary antibody (Molecular Probes, Eugene, OR) was used at 1:1,000 dilution. DNA was counterstained with DAPI III (Vysis, Abbott Park, IL) and cells were observed under immunofluorescence microscopy (Leica QFISH; Leica Microsystems, Tokyo, Japan).

3.4. Apoptosis detection

Apoptotic cells were detected by TUNEL assay according to the manufacturer's instructions (Apoptosis Detection System, Fluorescein. Promega, WI, USA). Briefly, HeLa cells cultured on cover glasses were fixed with paraformaldehyde at 4°C for 10 min on ice and permeabilized with 0.5% Triton-X-100 solution in PBS for 5 min. After washing with PBS twice, apoptotic cells were visualized through detection of inter-nucleosomal fragmentation of DNA using *in situ* nick-end labeling with terminal deoxynucleotidyl transferase (TdT) and FITC-labeled dUTP (MEBSTAIN Apoptosis Kit: Medical & Biological Laboratories, Japan). DNA was counterstained either with DAPI III for microscopy.

3.5. Protein extraction and immunoblotting

Frozen tissue samples were dissolved in lysis buffer (7M urea, 2M thiourea, 2% 3-[(3-Cholamidopropyl) dimethylammonio-] 1-propanesulfate (CHAPS), 0.1 M Dithiothreitol (DTT), 2% IPG buffer (Amersham Pharmacia Biotech, Buckinghampshire, UK), 40 mM Tris) using a Polytron homogenizer (Kinematica, Switzerland) following centrifugation (100,000 x g) for 1hr at 4°C. The amount of protein in the supernatant was measured by protein assay (Bio-Rad, Hercules, CA). The proteins were separated by electrophoresis on 8 % polyacrylamide gels and transferred to a polyvinylidene fluoride membrane (Millipore, Bedford, MA) in a tank transfer apparatus (Bio-Rad, Hercules, CA). The membrane was blocked with 5% skim milk in PBS for 1hr. Rabbit polyclonal anti-FIR antibody and goat polyclonal anti-beta-actin antibody (Santa Cruz, Santa Cruz, CA) diluted 1:1,000 and 1:500, respectively, in blocking buffer were used as primary antibodies. Goat anti-rabbit IgG horseradish peroxidase conjugate (HRP) (Jackson, West Grove, PA) diluted 1:3,000 and rabbit anti-goat IgG HRP (Cappel, West Chester, PA) diluted 1:500 were used as secondary antibodies. Antigens on the membrane were detected by ECL™ detection reagents (Amersham Pharmacia Biotech). The intensity of each band was measured by NIH Image.

3.6. Reverse transcriptase (RT)-PCR and real-time quantitative PCR

Total RNA and genomic DNA were extracted from tumor and non-tumor epithelial tissues with the RNeasy™ Mini Kit and the DNeasy™ Tissues Kit (Qiagen). cDNA was synthesized from total RNA with the 1st strand cDNA Synthesis Kit for RT-PCR (Roche, Mannheim, Germany). Using the cDNA as a template, FIR cDNA was amplified with suitable primers by RT-PCR: forward 5'-GGCCCCATCAAGAGCATC -3', reverse 5'-GGGGCTGGGCCAGGGTCAG -3'. For control, GAPDH cDNA was amplified. The amino terminal region of FIR was amplified by RT-PCR with primers: forward 5'-AGACAGCGGAAGGAGCAAGAGTGG-3', reverse 5'-CTGTGCAGCTTCGGGGACCTCATA -3'. The PCR product was loaded on a 2.5 % agarose gel (Promega, WI), purified by Gel Extraction Kit™ (Qiagen) and cloned with the pGEM®-T Easy vector system (Promega, WI) for DNA sequencing.

3.7. MTT assay

The effects of FIR on cell survival were examined by the MTT method of Mosmann (11) as described previously (12). HeLa and esophageal squamous cell carcinoma cells (T.Tn) were infected with Ad-FIR or control Ad-LacZ at MOI 0.1 to 10, and cultured for 3 days. Cell viability was quantified by measuring the absorbance at 570 nm after incubation with MTT for 4 hr. The results are shown as percentages of the control results.

3.8. FIR adenovirus vector

The recombinant adenoviral vectors that express FIR was constructed through homologous recombination in Escherichia coli using the AdEasy XL system (STRATAGENE, Cedar Creek, Texas). *Hind*III-*Pme*I fragment of pcDNA3.1-FIR or *Hind*III-*Eco*RV fragment of pcDNA3.1-CMV-LacZ were cloned into the *Hind*III–*Eco*RV sites of pShuttle-CMV, generating pShuttle-CMV-FIR or pShuttle-CMV-LacZ, respectively. The resultant shuttle vectors were linearized with *Pme*I digestion and subsequently cotransfected into *Escherichia coli* BJ5183-AD-1. The recombinants were linearized with *Pac*I digestion and transfected into the E1 trans-complementing 293 cell line to generate Ad-FIR and Ad-LacZ. The viruses were propagated in the adenovirus packaging 293 cell line, and purified by double CsCl density gradient centrifugation, followed by dialysis against 10 mM Tris buffer (pH 8.0) with 10% glycerol. The viruses were aliquoted and stored at −80°C until usage. The virus titer was determined by conventional limiting dilution on 293 cells.

3.9. Tumor xenografts in animal model experiments

The *in vivo* inhibition of tumorigenicity of esophageal squamous cell carcinoma cells (TE-2) was examined by Ad-FIR or Ad-LacZ injection. $5x10^6$ cells of TE-2 inoculated with Ad-FIR or Ad-LacZ at an MOI of 10, were injected beneath the skin of right thigh of nude mice (balbc/nu/nu, 6-week birth, male). Tumor growth was observed and measured the long and short diameter for tumor volume calculation. Thirty days after inoculation, tumor grew up to 5-8 mm in diameter in 9 of 9 mice (100%).

4. RESULTS

4.1. The amino terminal domain of FIR is required to represses endogenous c-Myc expression.

Previous studies revealed that the amino terminus of FIR was necessary to repress transcription from the *c-myc* promoter of a transfected reporter plasmid (10). To test the effect of FIR on the endogenous c-Myc expression, HA-tagged, full length FIR (HA-FIR) was expressed in HeLa cells, the transfected cells were identified using anti-HA and c-Myc expression in transfected cells was visualized by immunostaining with anti-c-Myc (Figure 1A upper panels). c-Myc levels were greatly diminished in HA-FIR expressing cells (arrowheads), but were unperturbed in HA-negative cells, demonstrating that FIR represses endogenous c-Myc expression through a cell autonomous mechanism. To test if the amino-terminal region of FIR is required for the suppression of c-Myc, its amino terminal deletion mutant (HA-FIRdel/N77) was transfected into HeLa cells (Figure 1A lower panels). In contrast to the full-length protein, deleting its amino-terminus enfeebled FIR's repressor activity (arrows).

4.2. FIR-induced apoptosis is prevented by enforced expression of c-Myc.

Because FIR depresses native *c-myc* expression, we tested the influence of enforced FIR-expression upon apoptosis. HA-FIR and HA-FIRdel/N77 were transfected into HeLa cells and apoptosis was examined by TUNEL assay (Figure 1B). HA-FIR induced apoptosis with DNA fragmentation (Figure 1B upper panel with arrows), whereas little apoptosis occurred in cells transfected with HA-FIRdel/N77 or the control vector. Equivalent expression of HA-FIR and HA-FIRdel/N77 protein in HeLa cells was confirmed by immunoblot (data not shown).

If FIR suppression of *c-myc* drives apoptosis, then bypassing this repression should rescue cells from death. Expression from an exogenous promoter enabled the elevation of c-Myc levels even when co-transfected with FIR (Figure 1C right upper panel; arrowheads). Augmented c-Myc expression protected HeLa cells from the FIR-driven apoptosis. The extent of apoptosis driven by FIR declined from 21.1% to 4.2% when c-Myc expression was enforced (Figure 1D). The elevating c-Myc levels also prevented FIR-induced nuclear swelling and degradation (Figure 1C right lower panels). These results indicate that increasing FIR levels, triggers apoptosis, most likely due to *c-myc* suppression.

4.3. FIR is paradoxically upregulated in colorectal cancer correlating with increased c-Myc.

It is well known that c-Myc is overexpressed in the majority of colorectal cancers due to deregulation of *c-myc* expression. Thus we hypothesized that cancer cells must escape FIR-repression of *c-myc*. FIR itself might be downregulated in cancer, or alternatively the effector actions of FIR in transcription and apoptosis might be disabled. To test if FIR is downregulated in colorectal cancer, FIR protein levels in tumors and normal tissue from 10 cases were examined by immunoblot. Unexpectedly,

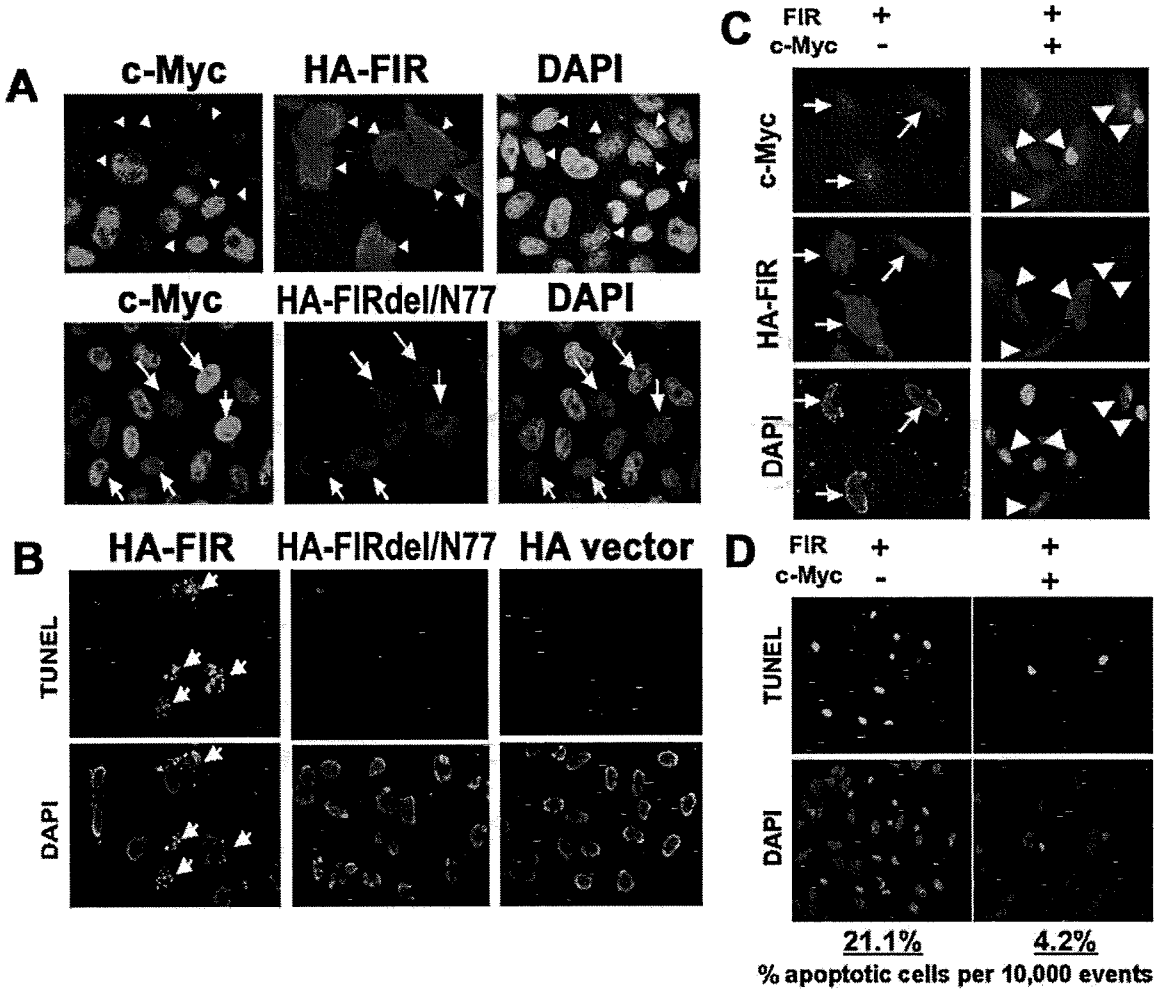

Figure 1. FIR suppresses c-Myc and induces apoptosis; the amino terminus is necessary for the activities. (A) 100 fmol of HA-FIR or HA-FIRdel/N77 was transfected into HeLa cells in 6-well plate. After 24 hours, cells were immunostained with antibodies against c-Myc (left, green) or HA (middle, red). Arrowheads and arrows show the cells in which HA-FIR and HA-FIRdel/N77 were expressed, respectively. c-Myc expression was markedly reduced in most HA-FIR-expressing cells (arrowheads) when compared to HA-FIRdel/N77-expressing cells (arrows). (B) Examination of apoptotic cells by TUNEL assay. 150 fmoles of HA-FIR, HA-FIRdel/N77, vacant vector plasmids were transfected to HeLa cells in 6-well plate and 48 hours later TUNEL assay was performed. Upper panels show apoptotic cells (arrows) after HA-FIR transfection to HeLa cells. Middle and right panels are HA-FIRdel/N77 and control (HA vacant vector) transfected cells, respectively. (C) 600ng of pcDNA3.1-FIR were transfected into semiconfluent HeLa cells on a 6-well plate with or without 60 ng of c-Myc expression plasmids (pcDNA3.1-*c-myc*). c-Myc expression was remarkably suppressed when FIR alone was transfected (left, top, arrows) whereas overall c-Myc expression was elevated when *c-myc* plasmids were cotransfected with FIR plasmids (right, top, arrowheads). Staining with DAPI showed that nuclei were swollen and degraded in FIR transfected cells (left, bottom, arrows), vs. normal appearing in FIR and c-Myc co-expressing cells (right, bottom, arrowheads). (D) The number of apoptotic cells caused by FIR was drastically reduced when co-expressed with c-Myc. The percentage of apoptotic cells caused by FIR alone was 21.1%, but decreased to 4.2 % when FIR and c-Myc were co-expressed.

FIR levels were actually increased in most colorectal cancer tissue compared with the corresponding non-tumor epithelium (Figure 2A). To determine if the increased FIR levels resulted from increased levels of FIR mRNA, RNA from colorectal cancer cells and normal colonic epithelium were examined by RT-PCR (Figure 2B). All cases, except Case 2, showed higher FIR mRNA levels in tumors compared with non-tumor tissue. FIR mRNA and protein levels paralleled each other in all cases.

4.4. An alternatively spliced form of FIR is expressed in tumors, but not the adjacent normal tissue

Either FIR must be defective, or the *c-myc* promoter must somehow be made resistant to FIR. RT-PCR of full-length FIR cDNAs isolated from HeLa cells or colorectal cancer tissues using primers to amplify the amino terminal

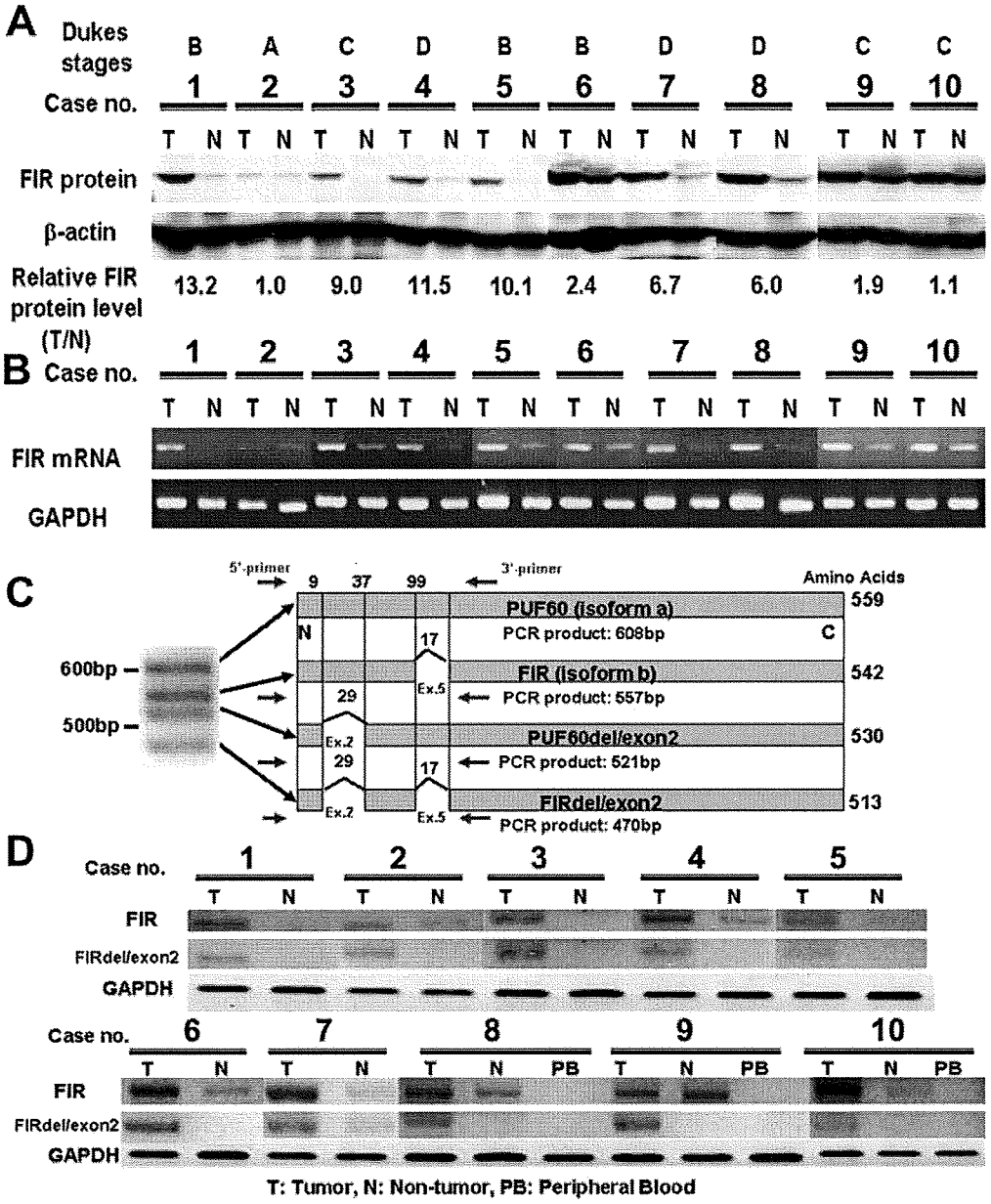

Figure 2. FIR was paradoxically overexpressed in colorectal cancer tissues. (A) Total protein lysates were prepared from matched samples of tumor (T) and adjacent non-tumor epithelial tissue (N). Equal amounts of protein from each pair were resolved on 8% polyacrylamide gel and immunoblotted with anti-FIR antibody. Immunoblotting was also performed with β-actin antibody as a loading control. Intensity of each band was measured by NIH Image and the relative mean of FIR protein levels between (T) and (N) with β-actin were calculated at the bottom of the figure. FIR expression significantly increased in (T) compared with corresponding (N). (B) Total RNAs were prepared from matched samples of (T) and (N) and RT-PCR was performed. FIR mRNA levels were comparative with the protein levels of each case. GAPDH mRNA levels are also showed as internal control. (C) Alternative spliced form of FIR that lacks exon 2 (FIRdel/exon2) is expressed specifically in human colorectal cancer tissues. FIR cDNA, obtained from HeLa cells or colorectal cancer tissues, was amplified by PCR using primers for the amino terminal region of FIR. Four distinct bands were observed in 2.5% agarose gel. Each band was excised and DNA was eluted, then sequenced. The PCR products were four alternative spliced forms of FIR that lack exon 2 and/or exon 5, whose sizes were 608bp, 557bp, 521bp, and 470bp, respectively. Exon 2 and exon 5 consists of twenty-nine and seventeen amino acids. Exon 2 locates at amino terminal suppression domain. (D) RT-PCR using cDNA obtained from colorectal cancer tissues was performed as in (A). Although both FIR and FIRdel/exon2 expressions increased in (T) compared with (N), FIRdel/exon2 was only expressed in tumor of all cases.

region revealed the four variants (Figure 2C; FIR and PUF60, FIRdel/exon2 and PUF60del/exon2) expected from the alternative utilization of the two optional exons. DNA sequencing confirmed that the four products reflected all combinations of inclusion/exclusion of exons 2 and 5 (Figure 2C). To examine if the alternative splicing of FIR is a tumor specific event, FIR cDNA isolated from tumors and normal tissues of several cases were examined by RT-PCR. The splicing variant FIRdel/exon2 was only observed in tumor tissues and not in adjacent normal tissues or in blood cells from most of the matched cases (Figure 2D).

4.5. FIR adenovirus indicates antitumor effect on human cancer cells *in vitro* and *in vivo*

Based on the concept of genetic alteration in carcinogenesis, gene therapy has increasingly developed as an alternative to conventional cancer therapy. We have previously reported that FIR induces apoptosis thus applicable for cancer gene therapy (10). Clinically, the recombinant adenoviral vector is expected to be a good agent for introducing genes of interest into cancer cells due to its high transduction efficiency. In this study, preclinical studies of adenoviral-mediated FIR gene delivery are required to confirm the anti-cancer effect *in vivo* and *in vitro*.

The effects of FIR on the survival of cervical squamous cell carcinoma (HeLa), and esophageal cancer cells (T.Tn) were examined by infection with Ad-FIR followed by MTT assay. The viability of Ad-FIR-infected cells were much lower than that of control Ad-LacZ-infected cells at each MOI ranging from 0.1 to 10. This difference may be attributed to the expression of FIR. Almost complete loss of surviving cells by infection with Ad-FIR at an MOI of 10 suggests the cytocidal effects of FIR. The suppression of the viability was more prominent to HeLa cells than to T.Tn cells, possibly reflecting the protein expression levels of FIR. The growth of TE-2 cells injected into nude mice was also suppressed by infection with Ad-FIR. Significant growth retardation was observed with Ad-FIR but not with control Ad-LacZ (data not shown).

In the above set of experiments, we demonstrated that adenovirus-mediated FIR gene transduction efficiently suppressed tumor growth of human cancer cell lines both *in vitro* and *in vivo*. Precise determination of the mechanism underlying the growth suppressive effect by FIR will require further investigation.

5. DISCUSSION

In this study, FIR adenovirus vector significantly inhibited tumor growth in mice animal model. The mechanism of anti-tumor effect by overexpression of FIR recombinant adenovirus vector (Ad-FIR) appears to be the induction of apoptosis. We herein report the findings of a preclinical study that reveal the efficacy of Ad-FIR treatment on human cancers both *in vitro* and *in vivo*. Tumor cells inoculated with Ad-FIR demonstrated significant growth retardation at an MOI of 10. This strategy could be useful for patients to whom relatively curative resection has been performed for locally advanced cancers and possible micro residual cancers are present.

This study demonstrated that FIR strongly repressed endogenous *c-myc* transcription and induced apoptosis. Most importantly, a splicing variant of FIR, FIRdel/exon2, found frequently in human primary colorectal cancer tissues, not only lacked the c-Myc-suppressing and apoptosis-inducing action of FIR, but prevented normal FIR from performing these activities. Thus FIRdel/exon2 may contribute to tumor progression by enabling higher levels of *c-myc* expression and greater resistance to apoptosis in tumors than in normal cell (Figure 3A). Though splice variants can function as dominant negative inhibitors and interfere with the wild type, their selective occurrence in tumors has not been proven. To demonstrate how the alternative splicing of FIR is differentially regulated between tumors and the surrounding normal tissue promises to expose further links between the earliest events in carcinogenesis with tumor progression. In addition FIR and/or FIRdel/exon2 are elevated in colorectal cancer tissues, circulating FIR and/or FIRdel/exon2 proteins or mRNAs in peripheral blood are potent biomarker for cancer detection. The value of FIR and/or FIRdel/exon2 detection for cancer diagnosis is under investigation.

Our experiments indicate that the FIR is an important player in these processes by directly regulating *c-myc*. Evidence for this scheme includes: 1) the amino terminus of FIR, essential for *c-myc* suppression, is also necessary for induction of apoptosis. 2) a splicing variant of FIR lacking exon 2 in the amino terminus failed not only to suppress c-Myc expression but to induce apoptosis. 3) enforced expression of c-Myc rescued cells from FIR-induced apoptosis. Together, FIRdel/exon2 protein transport inhibition into the nucleus and/or FIRdel/exon2 mRNA export inhibition into the cytoplasm may be promising molecular targets for future cancer therapy (Figure 3B).

Recently, Puf60, another FIR splicing variant having exon 5, directly binds to splicing factor SF3b with $U2AF^{65}$ (13, 14) and inhibition of SF3b by natural chemicals demonstrated strong antitumor effect (15, 16). Given the central role of c-Myc in the development of many cancers and inhibition of splicing function of FIR homologue (or FIR itself) with SF3b indicates strong antitumor activity, one route to the development of cancer therapies directed against c-Myc and splicing of SF3b inhibition may go through FIR and its variants (Figure 3B). Further studies are required in this field.

According to recent cancer gene therapy reports, adenovirus-mediated p53 gene transfer is frequently used, together with cis-dichloro-diammineplatinum (CDDP) administration or ionizing radiation (17). As for Ad-FIR vector, the transduction efficiency was relatively low, but an MOI of 10 was sufficient to show the efficacy in preclinical trials. Because treatment

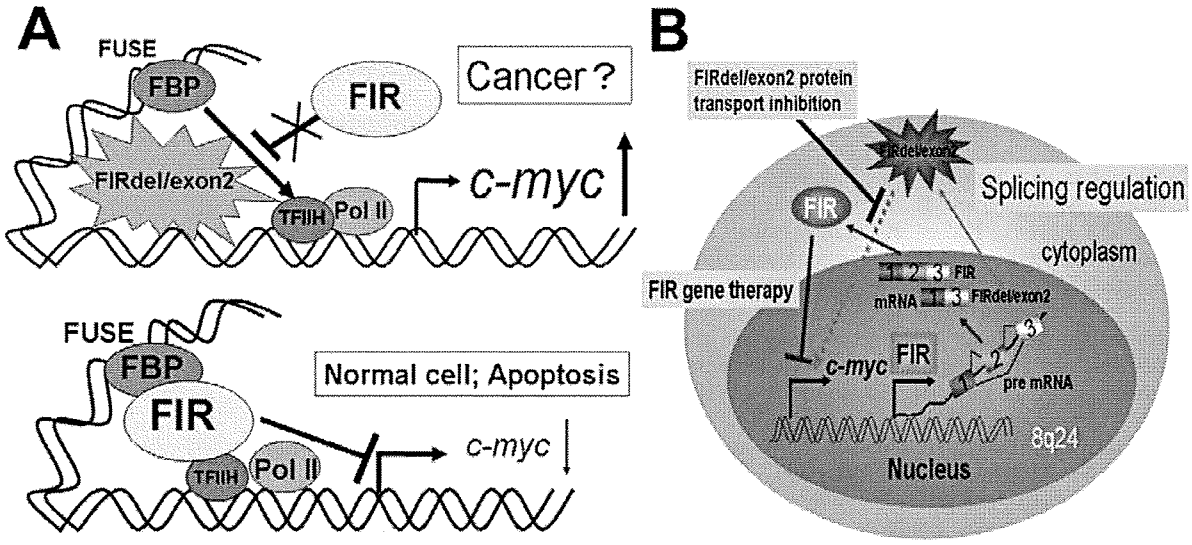

Figure 3. (A) c-Myc plays a critical role in cell proliferation and tumorigenesis. The Far UpStream Element (FUSE) is a sequence required for proper expression of the human *c-myc* gene. The FUSE is located 1.5 kb upstream of *c-myc* promoter P1, and binds the FUSE Binding Protein (FBP), a transcription factor stimulating *c-myc* expression in a FUSE dependent manner. FIR interacts with the central DNA binding domain of FBP. FIR was found to engage the TFIIH/p89/XPB helicase of TFIIH and repress *c-myc* transcription by delaying promoter escape. In this study, we show that a splice variant of the *c-myc* repressor FIR plays an important role in the pathogenesis of human colorectal cancer. A FIRdel/exon2, existing only in tumors, but not in the adjacent normal tissue, failed to repress c-Myc and inhibited FIR-induced apoptosis suggesting an important role for this splicing variant of FIR in the tumorigenesis of human colorectal cancer. (B) FIR gene therapy is a promising tool for cancer treatment. FIRdel/exon2 protein transport inhibition into the nucleus and/or FIRdel/exon2 mRNA export inhibition into the cytoplasm may be potential molecular targets for future cancer therapy leading *c-myc* suppression. FIR and/or FIRdel/exon2 mRNAs in the peripheral blood are potent biomarkers for cancer detection.

response is strongly associated with survival, combination treatment with standard chemoradiation and Ad-FIR may be an attractive modality in the future. FIR and its splicing variants are fascinating targets for cancer diagnosis and treatment.

6. ACKNOWLEDGEMENTS

This work was supported in part by a Grant-in-Aid 18591453 to K.M and by the 21st Century COE (Center Of Excellence) Programs to T.O. from the Ministry of Education, Science, Sports and Culture of Japan.

7. REFERENCES

1. Suntharalingam, M, J., Moughan, L.R., Coia, M.J., Krasna, L., Kachnic, D.G., Haller, C.G., Willet, M.J., John, B.D., Minsky and Owen, J.B.: Outcome results of the 1996-1999 patterns of care survey of the national practice for patients receiving radiation therapy for carcinoma of the esophagus. *J Clin Oncol* 23, 2325-2331 (2005)

2. Stahl, M, M., Stuschke, N., Lehmann, H.J., Meyer, M.K., Walz, S., Seeber, B., Klump, W., Budach, R., Teichmann, M., Schmitt, G. et al: Chemoradiation with and without surgery in patients with locally advanced squamous cell carcinoma of the esophagus. *J Clin Oncol* 23, 2310-2317 (2005)

3. Pelengaris, S., Khan, M., and Evan, G. I: Suppression of Myc-induced apoptosis in beta cells exposes multiple oncogenicproperties of Myc and triggers carcinogenic progression. *Cell* 109, 321-334 (2002)

4. Matsushita, K., Takenouchi, T., Shimada, H., Tomonaga, T., Hayashi, H., Shioya, A., Komatsu, A., Matsubara, H., and Ochiai, T. Strong HLA-DR antigen expression on cancer cells relates to better prognosis of colorectal cancer patients: Possible involvement of c-myc suppression by interferon-gamma in situ. *Cancer Sci* 97, 57-63 (2006)

5. Bazar, L., Meighen, D., Harris, V., Duncan, R., Levens, D., and Avigan, M: Targeted melting and binding of a DNA regulatory element by a transactivator of c-myc. *J Biol Chem* 270, 8241-8248 (1995)

6. Michelotti, G. A., Michelotti, E. F., Pullner, A., Duncan, R. C., Eick, D., and Levens, D: Multiple single-stranded cis elements are associated with activated chromatin of the human c-myc gene in vivo. *Mol Cell Biol* 16, 2656-2669 (1996)

7. Liu, J., Akoulitchev, S., Weber, A., Ge, H., Chuikov, S., Libutti, D., Wang, X. W., Conaway, J. W., Harris, C. C., Conaway, R. C., et al: Defective interplay of activators and repressors with TFIH in xeroderma pigmentosum. *Cell* 104, 353-363 (2001)

8. Black, D. L: Mechanisms of alternative pre-messenger RNA splicing. *Annu Rev Biochem* 72, 291-336 (2003)

9. Brinkman, B. M: Splice variants as cancer biomarkers. *Clin Biochem* 37, 584-594 (2004)

10. Matsushita, K., Tomonaga, T., Shimada, H., Higashi, M., Shioya, A., Matsubara, H., Harigaya, K., Nomura, F., Libutti, D., Levens, D., et al.: An essential role of alternative splicing of c-myc suppressor FIR in carcinogenesis. *Cancer Res* 66, 1409-1417 (2006)

11. Mosmann, T.: Rapid colorimetric assay for cellular growth and survival: application to proliferation and cytotoxicity assays. *J Immunol Methods* 65, 55-63 (1983)

12. Hiwasa, T., Shimada, H., Sakaida, T., Kitagawa, M., Kuroiwa, N., Ochiai, T. and Takiguchi, M.: Drug-sensitivity pattern analysis of study of functional relationship between gene products. *FEBS Lett* 552, 177-183 (2003)

13. Corsini, L., Hothorn, M., Stier, G., Rybin, V., Scheffzek, K., Gibson, T.J., and Sattler, M. Dimerization and protein binding specificity of the U2AF homology motif (UHM) of the splicing factor Puf60. *J Biol Chem* (2008) [Epub ahead of print]

14. Hastings, M.L., Allemand, E., Duelli, D.M., Myers, M.P., and Krainer, A.R. Control of pre-mRNA splicing by the general splicing factors PUF60 and U2AF^{65}. *PLosONE* 2, e538 (2007)

15. Kotake, Y., Sagane, K., Owa, T., Mimori-Kiyosue, Y., Shimizu, H., Uesugi, M., Ishihama, Y., Iwata, M., and Mizui, Y. Splicing factor SF3b as a target of the antitumor natural product pladienolide. *Nat Chem Biol* 3, 570-5 (2007)

16. Kaida, D., Motoyoshi, H., Tashiro, E., Nojima, T., Hagiwara, M., Ishigami, K., Watanabe, H., Kitahara, T., Yoshida, T., Nakajima, H., et al. Spliceostatin A targets SF3b and inhibits both splicing and nuclear retention of pre-mRNA. *Nat Chem Biol* 3, 576-83 (2007)

17. Swisher, S.G., Roth, J.A., Komaki, R., Gu, J., Lee, J.J., Hicks, M., Ro, J.Y., Hong, W.K., Merritt, J.A., Ahrar, K., et al: Induction of p53-regulated genes and tumor regression in lung cancer patients after intratumoral delivery of adenoviral p53 (INGN 201) and radiation therapy. *Clin Cancer Res* 9, 93-101 (2003)

Abbreviations: FUSE: Far Upstream Element; FBP: FUSE-Binding protein; FIR: FBP Interacting Repressor, Ad: adenovirus

Key Words: Cancer gene therapy, *c-myc* suppressor, FUSE-Binding Protein-interacting repressor, FIR, adenovirus vector

Send Correspondence to: Kazuyuki Matsushita. Department of Molecular Diagnosis, Graduate School of Medicine, Chiba University, 1-8-1 Inohana, Chuo-Ku,Chiba,260-8670, Japan, Tel: 81-43-222-7171 (ext. 5432), Fax: 81-43-226-2169, E-mail: kmatsu@faculty.chiba-u.jp

http://www.bioscience.org/current/vol14.htm

UICC
global cancer control

IJC
International Journal of Cancer

An alternative splicing isoform of eukaryotic initiation factor 4H promotes tumorigenesis *in vivo* and is a potential therapeutic target for human cancer

AQ1 Di Wu[1], Kazuyuki Matsushita[1], Hisahiro Matsubara[2], Fumio Nomura[1] and Takeshi Tomonaga[1,3]

AQ2 [1] Department of Molecular Diagnosis (F8), Graduate School of Medicine, Chiba University, Chuo-ku, Chiba, Japan
[2] Department of Frontier Surgery (M9), Graduate School of Medicine, Chiba University, Chuo-ku, Chiba, Japan
[3] Laboratory of Proteome Research, National Institute of Biomedical Innovation, Saito-Asagi, Ibaraki, Japan

Deregulation of protein synthesis plays a critical role in cell transformation. Several translation initiation factors (eIFs) have been implicated in malignant transformation; thus, suppression of eIFs could be a potential cancer therapy if cancer cells are selectively killed without damaging healthy cells. One of the potential molecular targets is a cancer-specific splicing variant. We have previously shown that one of the splicing variants of eIF4H (isoform 1) was overexpressed in primary human colorectal cancer. Our study aimed to explore whether eIF4H isoform 1 contributes to carcinogenesis and could be an efficient molecular target for human cancer therapy. We found that its overexpression in immortalized mouse fibroblasts, NIH3T3 cells, generated tumors in nude mice. Conversely, suppression of eIF4H isoform 1 expression using specific siRNA inhibited the proliferation of colon cancer cells *in vitro* and subcutaneously implanted tumor *in vivo*. Strikingly, eIF4H isoform 1 specific siRNA showed no effect on the growth of immortalized human fibroblasts. More interestingly, ectopic expression of eIF4H isoform 1 greatly increased the cyclin D1 level. On the other hand, cyclin D1 decreased by shRNA-mediated suppression of eIF4H isoform 1. Moreover, cotransfection of eIF4H isoform 1 siRNA and cyclin D1 expression plasmid was able to reverse the growth suppression effect of eIF4H isoform 1 knockdown. These results suggest that eIF4H isoform 1 plays an important role in carcinogenesis through the activation of oncogenic signaling and could be a promising molecular target for cancer therapy.

There is increasing evidence that deregulation of protein synthesis is associated with cell transformation and the malignant phenotype.[1–4] Protein synthesis is primarily regulated at the step of ribosome recruitment to the 5′-mRNA terminus and this association is mediated by a trimeric complex, termed eIF-4F, which consists of the large scaffolding protein eIF4G, the RNA helicase eIF4A, and the cap binding protein eIF4E. Several eIFs have been demonstrated to be involved in carcinogenesis. Overexpression of eIF4E, a subunit of the eIF-4F complex, has been observed in many solid tumors and tumor cell lines[1–5] and, in experimental models, it markedly alters cellular morphology, enhances proliferation and induces cellular transformation, tumorigenesis and metastasis.[6–8] Other members of the eIF-4F complex are also implicated in malignant transformation. For example, eIF4G is overexpressed in squamous cell lung carcinomas[9,10] and its overexpression in NIH3T3 cells leads to anchorage-independent growth of cells and tumor formation in nude mice.[11] eIF4A, an ATP-dependent RNA helicase, is also overexpressed in human melanoma cells and primary hepatocellular carcinomas.[12,13] eIF4H was first identified to stimulate translation in rabbit reticulocytes.[14] It has been recognized that eIF4H stimulates protein synthesis by enhancing the helicase activity of eIF4A by increasing the processivity of eIF4A.[14–16] We have previously reported that eIF4H was overexpressed in most human colorectal cancer tissues[17]; thus, it has become evident that control of mRNA translation plays a critical role in carcinogenesis. A likely mechanism of cellular transformation by eIFs has been suggested as increased translational efficiency of the mRNA responsible for the control of cell growth or

Key words: alternative splicing, translation initiation factor, therapeutic target

Abbreviations: CHAPS: 3-[(3-cholamidopropyl) dimethylammonio]-1-propanesulfonate; DTT: dithiothreitol; eIFs: eukaryotic initiation factors; FACS: fluorescence-activated cell sorting; IMDM: iscove's modified dulbecco's media; MTS: 3-(4, 5-dimethylthiazol-2-yl)-5-(3-carboxymethoxyphenyl)-2-(4-sulfophenyl)-2H-tetrazolium; RNAi: RNA interference; RPMI-1640: Roswell Park Memorial Institute media; shRNA: short hairpin RNA; TdT: terminal deoxynucleotidyl transferase; Tet-Off system: tetracycline-off system; TUNEL: terminal deoxynucleotidyl transferase-mediated dUTP nick end labeling assay

Additional Supporting Information may be found in the online version of this article.

Grant sponsor: Ministry of Education, Science, Sports and Culture of Japan; **Grant numbers:** 16390353, 17015007, 18058006, 19390330
DOI: 10.1002/ijc.25419
History: Received 2 Nov 2009; Accepted 12 Apr 2010; Online 00 Month 2010

Correspondence to: Takeshi Tomonaga, Laboratory of Proteome Research, National Institute of Biomedical Innovation, 7-6-8 Saito-Asagi, Ibaraki City, Osaka 567-0085, Japan, Tel.: 81-72-641-9861, Fax: 81-72-641-9861, E-mail: tomonaga@nibio.go.jp

J_ID: Z3Q Wiley Ed. Ref. No.: 09-2572.R2 Customer A_ID: IJC25419 Date: 12-May-10 Stage: Page: 2

apoptosis, although the precise mechanism of how these factors are involved in carcinogenesis remains to be established.

Alternative splicing has been observed in many cancer-associated genes, suggesting that it might have a key role in carcinogenesis.[18–21] Hence, cancer-specific spliced isoforms may be potential tools as tumor markers or for molecular treatments that can be designed to recognize only the variant form. The eIF4H gene is known to produce two splice variants, isoform 1 and 2 (exon 5 is alternatively spliced),[22] which generate two protein products, 27 kDa and 25 kDa. Between them, overexpression of isoform 1 is much more prominent than isoform 2 in colon cancers. In this regard, eIF4H isoform 1 might be a cancer-driving splice variant and therefore a promising therapeutic target.

In our work, we investigated whether the alternative splicing form of eIF4H contributes to cell proliferation and carcinogenesis. We showed that overexpression of eIF4H isoform 1 induces tumor formation in nude mice and its suppression inhibited cell proliferation *in vitro* and *in vivo*. The effect of eIF4H isoform 1 on proliferation is likely due to the upregulation of an oncogenic factor cyclin D1. Our results suggest that eIF4H isoform 1 might become an attractive target of therapeutic intervention for colon cancer.

Material and Methods

Human tissue samples

Tissues from 10 patients with primary colorectal and 20 patients with esophageal cancer (Table 1) were resected surgically in the Department of Frontier Surgery, Chiba University Hospital. The ethics committee of the Graduate School of Medicine, Chiba University approved the protocol. Written informed consent was obtained from each patient before operation. The percentage of tumor cells in the tissues was 50–80% in all cases. The excised samples were obtained within 1 hr after the operation from tumor tissues and the corresponding nontumor tissues of the same patients 5–10 cm from the tumor. All excised tissues were placed immediately in liquid nitrogen and stored at −80°C until analysis.

Cell culture

Two human colon cancer cell lines, LOVO and RKO, two human lung fibroblast cell lines, MRC5 and WI38, and a mouse fibroblast, NIH3T3, were purchased from RIKEN Cell Bank (Tsukuba, Japan). The tumor cells, LOVO and RKO, were grown in RPMI-1640, and immortalized cells, MRC5, WI38 and NIH3T3, were grown in IMDM medium, both supplemented with 10% fetal bovine serum (FBS), 1% (v/v) penicillin and streptomycin (100 U/ml) (all from Invitrogen, Carlsbad, CA), and maintained at 37°C in a 5% CO_2-95% air atmosphere.

Real-time quantitative PCR

Total RNA was extracted from tumor and nontumor tissues with an RNeasy Mini kit (Qiagen, Tokyo, Japan). Total RNA from the nucleus and cytoplasm of colon cancer cells was extracted with a Protein and RNA Isolation System (PARIS) Kit (Applied Biosystems Japan, Tokyo, Japan). cDNA was synthesized from total RNA with the first-strand cDNA synthesis kit for RT-PCR (Roche, Mannheim, Germany). Real-time quantitative PCR of eIF4H cDNA using the LightCycler

Table 1. Clinical features of patients with esophageal cancer and colorectal cancer

No.	Age	Sex	Location	Stage[1]	Histological type
Patients with esophageal cancer					
1	66	M	Mt/Ut	2a	Mod[2]
2	53	M	Ae	3	Mod[2]
3	67	M	Mt/Ut	4b	Well[2]
4	64	M	Ae	2a	Mod[2]
5	55	M	Mt	2a	Mod[2]
6	56	M	Ut/Mt	4b	Mod[2]
7	67	M	Lt	1	Mod[2]
8	63	M	Mt/Lt	4b	Mod[2]
9	62	M	Lt	3	Well[2]
10	55	M	Lt	2a	Well[2]
11	73	M	Lt	4a	Mod[2]
12	63	M	Lt/Ae	3	Mod[2]
13	71	M	Lt/Ae	3	Mod[2]
14	63	M	Lt/Ae	4b	Well[2]
15	64	M	Mt	3	Mod[2]
16	45	M	Lt/Ae/Mt	4b	Poor[2]
17	54	M	Ae	4a	Mod[2]
18	54	M	Lt/Ae	3	Well[2]
19	58	M	Lt/Ae	2a	Combined[2]
20	67	M	Lt/Ae	2a	Mod[2]
Patients with colorectal cancer					
6R	57	M	S	2	Well[3]
27R	51	M	R	4	Mod[3]
29R	51	M	R	3b	Mod/poor[3]
34R	59	M	R	3a	Well/mod/poor[3]
35C	72	F	S	2	Well[3]
36C	67	M	T	3a	Mod/poor[3]
37C	49	M	R	3a	Well[3]
112	72	M	S	3b	Mod[3]
117	49	M	Ce	4	Mod[3]
118	85	M	S	2	WELL[3]

[1]Stage is described according to Union Internationale Contre le Cancer (UICC) TNM Classification (Fifth Edition, 1997). [2]Well, well-differentiated squamous cell carcinoma; mod, moderately differentiated squamous cell carcinoma; poor, poorly differentiated squamous cell carcinoma; combined, combined squamous cell carcinoma with basaloid carcinoma. [3]Well, well-differentiated adenocarcinoma; mod, moderately differentiated adenocarcinoma; poor, poorly differentiated adenocarcinoma.Abbreviations: Ut: upper thoracic esophagus; Mt: middle thoracic esophagus; Lt: lower thoracic esophagus; Ae: abdominal esophagus; S: sigmoid colon; R: rectum; T: transverse colon; Ce: cecum.

ID: jaishankarn | Black Lining: [ON] | Time: 13:38 | Path: N:/3b2/IJC#/Vol00000/100296/APPFile/C2IJC#100296

instrument (Roche) was carried out in 20 μl of reaction mixture containing 2 μl of 10× LightCycler DNA Master SYBR Green I (FastStart Taq DNA polymerase, deoxynucleotide triphosphate, buffer, SYBR Green I), 3.0 mM $MgCl_2$ and 0.5 μM each of forward (5′-GGAAGCCTTGACATACGAT-3′), and reverse primer (5′-CATCCCTGAAGCCAGAAT-3′) in a LightCycler capillary. Real-time quantitative PCR of cyclin D1 cDNA was carried out in 20 μl of reaction mixture containing 2 μl of 10× LC FastStart DNA Master Hybridization Probes, 4.0 mM $MgCl_2$ and 0.5 μM each of forward (5′-CCC CAA CAA CTT CCT GTC CTA-3′) and reverse primer (5′-CTC CAG CAG GGC TTC GAT-3′) 0.3 μM of Fluorescein Probe (5′-AGG CAG TCC GGG TCA CAC TTG ATC ACT-3′-Fluorescein), 0.4 μM of LCRed Probe (5′-LCRed640-5′-TGG AGA GGA AGC GTG TGA GGC GGT A-3′-phosphorylation) in a LightCycler capillary. Serial dilutions of template cDNA were made for PCRs to optimize PCR products within the linear range. LightCycler software version 3.3 (Roche) was used for analysis of quantitative PCR.

Western-blot analysis

Frozen tissue samples were solubilized in lysis buffer (7 M urea, 2 M thiourea, 2% 3-[(3-cholamidopropyl) dimethylammonio]-1-propanesulfonate (CHAPS), 0.1 M dithiothreitol (DTT), 2% IPG buffer (Amersham Pharmacia Biotech, Buckinghamshire, UK), 40 mM Tris) using a Polytron homogenizer (Kinematica, Switzerland) followed by centrifugation (100,000*g*) for 1 hr at 4°C. Cultured cells were solubilized in SDS sample buffer (62.5 mM Tris-Cl pH6.8, 2% SDS, 20% glycerol, 0.2% bromophenol blue, 0.025% β-mercaptoethanol) and heated for 5 min at 100°C. After passing through 27G needles, the samples were centrifuged for 15 min at 15,000*g*. A 30-μg sample of total protein from each lysate was loaded and separated by electrophoresis on 10–20% gradient gels (Bio-Rad, Hercules, CA). The proteins were transferred to polyvinylidene fluoride membranes (Millipore, Bedford, MA) in a tank-transfer apparatus (Bio-Rad), and the membranes were blocked with 5% skim milk in PBS. Antibodies used include eIF4H (prepared by Japan Bio Services; diluted 1:500), cyclin D1 (Sigma, Japan; 1:1,000), ornithine decarboxylase (ODC; Sigma; 1:200), Bcl-XL (Sigma; 1:1,000), Bcl-2 (Sigma; 1:1,000) and c-Myc (Oncogene Research Products; 1:500). Goat anti-rabbit IgG horseradish peroxidase (Bio-Rad) diluted 1:3,000, mouse anti-rabbit IgG horseradish peroxidase (Bio-Rad) diluted 1:1,000 and rabbit anti-goat IgG horseradish peroxidase (Cappel, West Chester, PA) diluted 1:500 in blocking buffer were used as secondary antibodies. Antigens on the membrane were detected with enhanced chemiluminescence detection reagents (Amersham Pharmacia Biotech).

Plasmid transfection and establishment of eIF4H isoform 1 overexpressed stable NIH3T3 Tet-Off cell line

The Tet-off system utilizes the tetracycline-dependent transcriptional repression activity of tTA protein (BD Biosciences Clontech, Palo Alto, CA). The eIF4H isoform 1 cDNA, driven by a tTA-repressible CMV promoter element in a TRE-Tight plasmid (pTRE-Tight/eIF4H isoform 1), was constructed as follows. Full-length eIF4H isoform 1 was amplified by PCR using HeLa cDNA library as a template and cloned into the TRE-Tight vector plasmid (BD Biosciences Clontech). Plasmids were purified with an Endofree® Plasmid Maxi Kit (Qiagen) and the DNA sequences were verified. To generate the NIH3T3 Tet-Off stable cell line, pTet-Off plasmid (BD Biosciences Clontech) was transfected as described previously.[23,24] Briefly, NIH3T3 cells were plated in 6-well plates in IMDM containing 10% FBS without antibiotics one day before transfection so that they were at 70–90% confluence at the time of transfection. On the day of transfection, 4 μg plasmids and 10 μl Lipofectamine 2000™ (Invitrogen) were diluted in 250 μl Opti-MEM I Reduced-Serum Medium (Invitrogen), respectively. After 5-min incubation at room temperature, the diluted plasmids and Lipofectamine 2000™ were combined and then further incubated for 20 min at room temperature. Then, DNA-Lipofectamine 2000™ complexes were then added to each well and cells were incubated for 48 hr at 37°C in a CO_2 incubator. NIH3T3 cells, 5×10^4, transfected with pTet-Off plasmid were transferred to 10-cm dishes 48 hr after transfection, and 400 μg/ml geneticin (Invitrogen) and 1 μg/ml doxycycline (Dox) were added to complete medium containing IMDM, 10% FBS, 1% penicillin-streptomycin. The complete medium with geneticin was replaced every 4 days and fresh Dox was added every 2 days until geneticin-resistant colonies began to appear. At least 30 clones were screened to find the clone with the highest induction in the absence of Dox and with the lowest background. Once the NIH3T3 Tet-Off stable cell line was obtained, the eIF4H isoform 1-overexpressed stable NIH3T3 Tet-Off cell line was generated by transfecting pTRE-Tight/eIF4H isoform 1 plasmid and linear hygromycin marker (0.2 μg) into the cells. Stable clones were selected by adding 400 μg/ml hygromycin and 1 μg/ml Dox to the medium as described above.

Gene knockdown using siRNA and cotransfection of cyclin D1 expression plasmid

siRNA targeting eIF4H RNA were generated to reduce eIF4H expression. The target sequence for eIF4H siRNA was 5′-AACCCACAGAAGAGGAAAGAG-3′ (si102), which is common to two splice variants of eIF4H, and two eIF4H isoform 1 specific siRNA were 5′-AATGGGTAGCTCTCGA GAATC-3′ (si103), 5′-AATCTAGAGGTGGATGGGATT-3′ (si104) (Japan Bio Services, Saitama, Japan), and eIF4H isoform 2-specific siRNA was 5′-AUG ACA GAG GCU UCA GGG A-3′ (iGENE, Tokyo, Japan). Blast analysis (http://www.ncbi.nlm.nih.gov/BLAST/) did not reveal overlapping regions between target sequences and other human genes. Cyclin D1 expression plasmid (CCND1 Human cDNA Clone) was purchased from Origene (Rockville, MD). Transfection of siRNA and plasmid was performed using lipofectamin 2000™ as described above.

Establishment of eIF4H isoform 1 stable knockdown colon cancer cell line

The eIF4H shRNAs, siRNA oligonucleotides connected by a spacer sequence, were cloned into a pBAsi-hU6 Neo plasmid (Takara Bio; Japan), where eIF4H shRNAs were driven by a hU6 promoter. The resulting plasmids, pBAsi-hU6-eIF4H shRNAs, were then transfected into LOVO cells and eIF4H isoform 1 stable knockdown clones, sh103-1, sh103-2 and sh104, were selected by adding 400 μg/ml geneticin, as described above.

Proliferation assays

Viable cell number was assessed according to 3-(4,5-dimethylthiazol-2-yl)-5-(3-carboxymethoxyphenyl)-2-(4-sulfophenyl)-2H-tetrazolium (MTS) dye absorbance following the manufacturer's instructions (Promega, Madison, WI). Absorbance was measured using a Wallac 1420 ARVOsx Multilabel Counter (Perkin-Elmer, Tokyo, Japan). Experiments were repeated in eight parallel studies.

Cell cycle analysis

Cells were fixed in 70% ethanol and treated with 50 μg/ml propidium iodide (Wako, Japan) in the presence of 200 μg/ml RNase A. Then, cells were subjected to cell cycle analysis using fluorescence activated cell sorting (FACS) Caliber cytometer (Becton Dickinson, San Jose, CA). At least 10,000 cells were counted for each sample, and data were analyzed with a Cell Quest program (Becton Dickinson, San Jose, CA).

TUNEL assay

Apoptotic cells were detected by the TUNEL assay according to the manufacturer's instructions (Apoptosis Detection System, Fluorescein; Promega, WI). Briefly, cells cultured in 6-well plate were fixed with paraformaldehyde at 4°C for 10 min on ice and permeabilized with 0.5% Triton-X-100 solution in PBS for 5 min. After washing with PBS twice, apoptotic cells were visualized through the detection of internucleosomal fragmentation of DNA using *in situ* nick-end labeling with terminal deoxynucleotidyl transferase (TdT) and FITC-labeled dUTP (MEBSTAIN Apoptosis Kit; Medical & Biological Laboratories, Japan).

Subcutaneous injection of the cells and tumor formation in nude mice

Male BALB/c nude mice, 4–5 weeks of age, were subcutaneously injected with 1×10^6 LOVO cells or 6×10^5 NIH3T3 cells into the left leg. Tumor size was calculated using the formula $(ab^2)/2$, where a and b represent the larger and smaller diameters, respectively, and was monitored every 3 days.

Results

eIF4H isoform 1 was overexpressed in gastrointestinal cancers

eIF4H gene is known to produce two splice variants, isoform 1 and 2 (exon 5 is alternatively spliced), which generate two protein products, 27 kDa and 25 kDa. Between them, not isoform 2, but isoform 1 expression, was significantly increased in colorectal cancers.[17] We then investigated if this was true in other gastrointestinal cancers, such as esophageal cancer. Detailed information on the esophageal cancer and colorectal cancer cases is shown in Table 1. Total protein lysates were prepared from 20 matched samples of the tumor (T) and adjacent nontumor tissue (N) and the expressions of eIF4H isoforms were examined with anti-eIF4H antibody. We found that eIF4H isoform 1 protein, but not isoform 2, was greatly increased in most esophageal cancers compared with the corresponding nontumor tissues (Figs. 1*a* and 1*b*), although there were no striking correlations between patient's pathological data and the eIF4H isoform 1 expression level (Table 1). F1

We therefore decided to focus on eIF4H isoform 1 in further studies. To examine if the increase of eIF4H isoform 1 occurred at the mRNA level, a set of primers that specifically amplifies isoform 1 was designed and real-time quantitative RT-PCR was carried out using total RNA extracted from tumor and nontumor tissues of 20 esophageal and 10 colorectal cancer patients (Fig. 1*c*). The eIF4H isoform 1 mRNA level was significantly elevated in the tumors, indicating that overexpression of the eIF4H isoform 1 is regulated at the mRNA level, such as elevated transcription, mRNA stability or de-regulation of alternative splicing.

Overexpression of eIF4H isoform 1 in NIH3T3 cell leads to tumor formation in nude mice

To directly investigate the transforming potential of eIF4H isoform 1, we created NIH3T3 cell lines that overexpress eIF4H isoform 1 using a Tet-Off gene expression system. The NIH3T3 cell line, which expresses the tetracycline-controlled transactivator, was stably trasfected with the eIF4H isoform 1 expression plasmid under the control of the tetracycline-responsive promoter so that eIF4H isoform 1 was expressed only in the absence of doxycycline (Dox). The cells were then screened for inducible eIF4H isoform 1 protein expression by immunoblotting with anti-eIF4H antibody. Three stable clones, no. 9, 10 and 306, were obtained, in which eIF4H isoform 1 expression was greatly induced by Dox removal from the media (Fig. 2*a*). Strikingly, subcutaneous injection of these stable clones overexpressing eIF4H isoform 1 into nude mice formed tumors after 3.5 weeks, whereas control mice injected with NIH3T3 cells did not generate tumors (Figs. 2*b* and 2*c*). These results suggest that eIF4H isoform 1 possesses transforming activity *in vivo*. F2

Suppression of eIF4H isoform 1 inhibits proliferation of colon cancer cell lines

To further examine the involvement of eIF4H isoform 1 in cell proliferation and carcinogenesis, RNA interference (RNAi) was used to suppress eIF4H expression. Several siRNA were designed to target different regions of the eIF4H open reading frame (Supporting Information Figure 1). Among them, siRNA (si103 and si104) suppressed only isoform 1

J_ID: Z3Q Wiley Ed. Ref. No.: 09-2572.R2 Customer A_ID: IJC25419 Date: 12-May-10 Stage: Page: 5

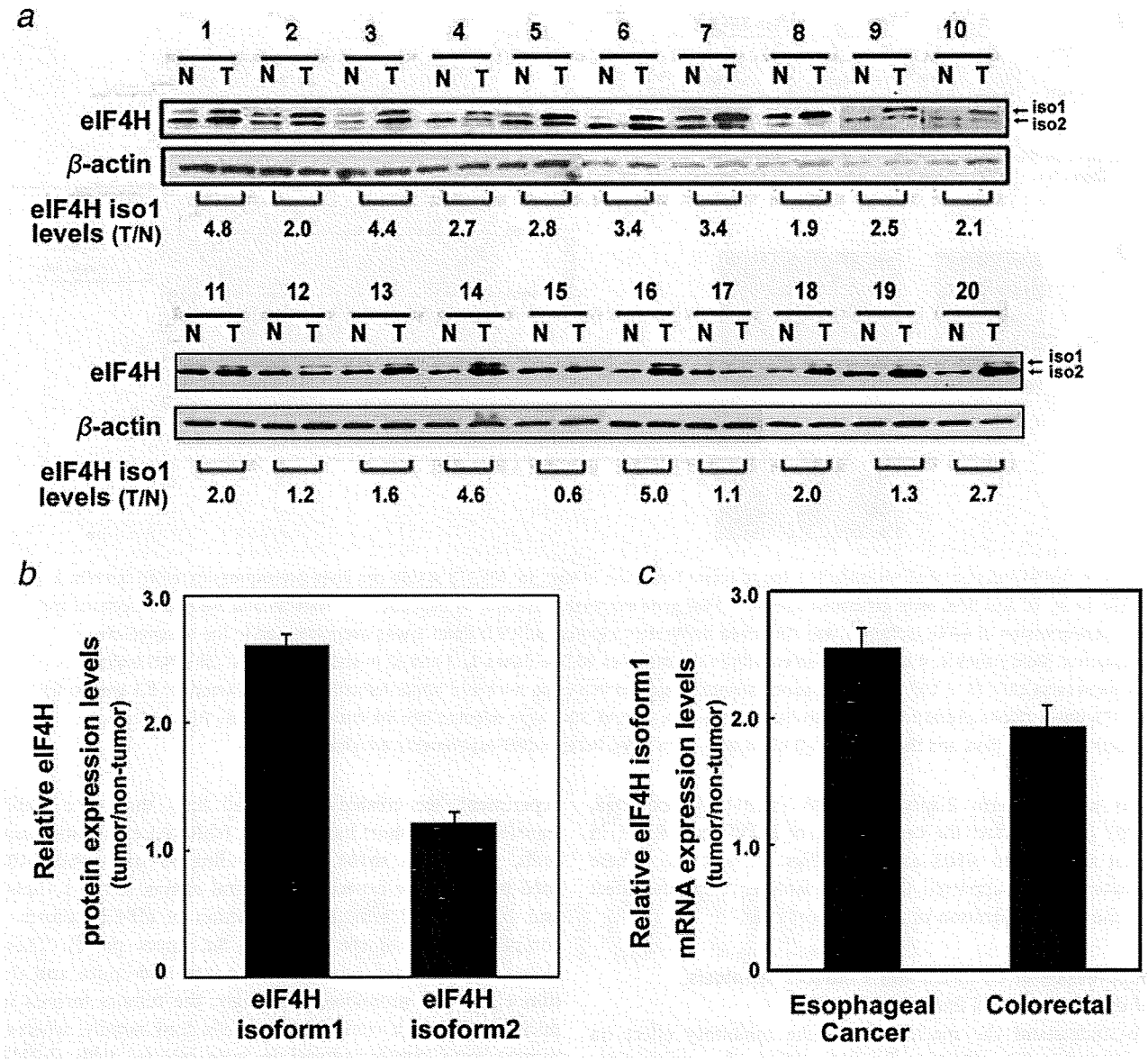

Figure 1. eIF4H isoform 1 was overexpressed in primary esophageal cancers tissues. (*a*) Total protein lysates were prepared from 20 matched samples of the tumor (T) and adjacent nontumor tissues (N). Equal amounts of protein from each pair were resolved on 10–20% gradient polyacrylamide gel and immunoblotted with anti-eIF4H and β-actin antibodies. Upper band: isoform 1; lower band: isoform 2. (*b*) The intensity of each band in (*a*) was measured with NIH Image and the mean ± SD of the relative eIF4H protein levels between tumor and nontumor tissue of 20 esophageal cancer patients normalized with β-actin were calculated. (*c*) Total RNA was prepared from matched samples of tumor and adjacent nontumor tissue of esophageal cancer and colorectal cancer patients, and real-time PCR was performed to examine the eIF4H isoform 1 mRNA level. Mean ± SD of relative eIF4H mRNA levels between tumor and nontumor tissue of 20 esophageal and 10 colorectal cancer patients normalized with β-actin were calculated.

and si201 suppressed only isoform 2 expression 48 hr after siRNA treatment in two colon cancer cell lines, LOVO and RKO (Figs. 3*a* and 3*b*); therefore, these three eIF4H siRNA (si103, 104 and 201) were used for further analysis.

To investigate the effect of eIF4H suppression on cell growth, the MTS assay was performed 48 hr after siRNA treatment of LOVO and RKO (Figs. 3*c* and 3*d*). Surprisingly, the suppression of eIF4H isoform 1 alone, using si103 and si104, strongly decreased the viable cell number by 30–50% as compared with the control. A similar decrease of the cell number was observed in RKO cells. These results imply that eIF4H isoform 1 plays an important role in the proliferation of colon cancer cells. Next, we examined if the suppression of eIF4H isoform 2 inhibits the proliferation of colon cancer

ID: jaishankarn | Black Lining: [ON] | Time: 13:38 | Path: N:/3b2/IJC#/Vol00000/100296/APPFile/C2IJC#100296

J_ID: Z3Q Wiley Ed. Ref. No.: 09-2572.R2 Customer A_ID: IJC25419 Date: 12-May-10 Stage: Page: 6

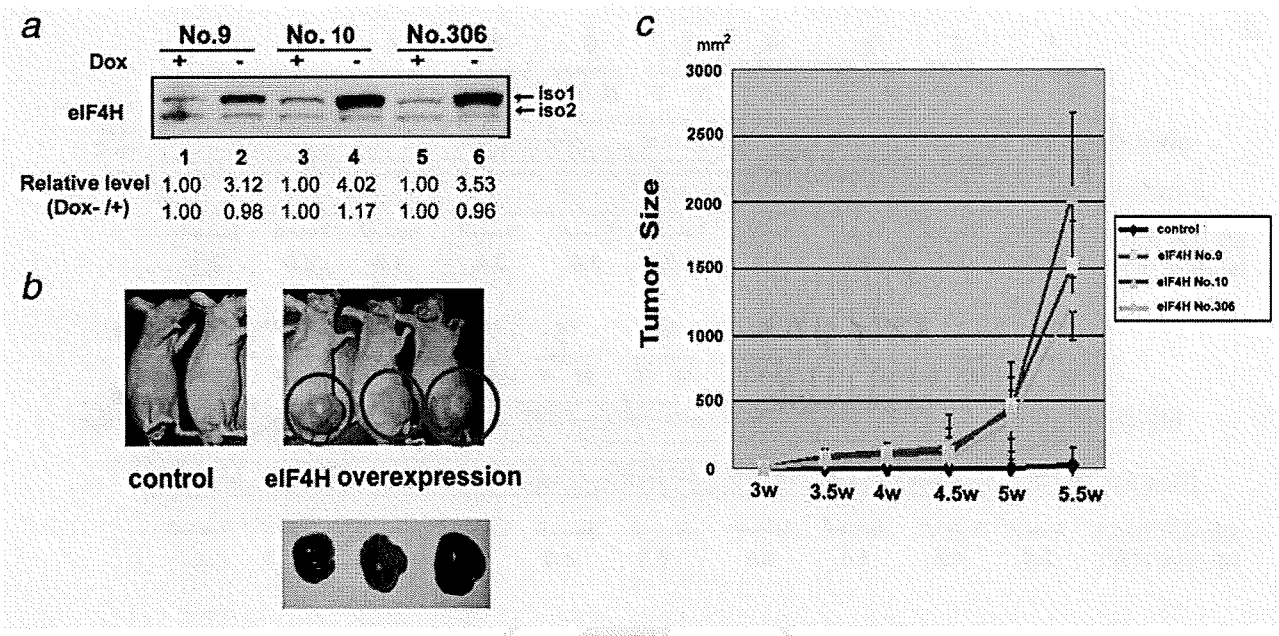

COLOR

Figure 2. Overexpression of eIF4H isoform 1 led to tumor formation *in vivo*. (*a*) NIH3T3 stable cell lines overexpressing eIF4H isoform 1 (clone no. 9, 10 and 306) were generated using a Tet-Off gene expression system, as described in "Material and Methods" section, and the overexpression of eIF4H isoform 1 was confirmed by Western blotting. eIF4H isoform 1 was overexpressed in the absence of doxycycline (Dox) (lanes 2, 4 and 6) compared with in the presence of Dox (lanes 1, 3 and 5) in stable cell lines. (*b*) eIF4H isoform 1-overexpressing cells (6×10^5 cells) were subcutaneously injected into nude mice and tumor formation was examined for 5.5 weeks. (*c*) NIH3T3 stable clones overexpressing eIF4H isoform 1, no. 9, 10 and 306, were injected into six mice, respectively. Tumor size was measured every 3 days and the mean ± SD of six mice from three independent experiments are shown.

Cancer Cell Biology

cells using isoform 2-specific siRNA (si201). As expected, si201 did not affect the cell number of LOVO and RKO, in great contrast to si103 and 104 (Figs. 3*c* and 3*d*). These results further supported the eIF4H isoform 1-specific effect on the cell proliferation of colon cancer cells.

Suppression of eIF4H isoform 1 induces apoptosis of colon cancer cell lines

To understand the mechanism of the inhibitory effect on proliferation by eIF4H isoform 1 siRNA, flow cytometric analysis was performed. The treatment of cells with si103 caused a 3-fold increase in the sub-G1 cell population and a decrease in the S phase compared with control cells, which suggests that the growth inhibition of cells by RNAi is due to the induction of apoptosis (Fig. 4*a*). This apoptosis was further confirmed by TUNEL assay (Fig. 4*b*). Both LOVO and RKO treated with si103 showed 60–70% of TUNEL-positive cells compared with about 20% in untreated control cells (Student's *t*-test, $p < 0.05$) (Fig. 4*c*). These results suggest that inhibition of apoptosis might be involved in the transforming activity of eIF4H isoform 1.

Suppression of eIF4H isoform 1 inhibited tumor growth in nude mice

Next, we investigated whether the suppression of eIF4H isoform 1 could also inhibit tumor growth *in vivo*. For the experiment, we created LOVO cell lines that were stably transfected with short hairpin RNA (shRNA) expression plasmids, sh103 and sh104, corresponding to si103 and si104 used in the above experiment. Several clones, sh103-1, 103-2 and 104, showed remarkable reduction of eIF4H isoform 1 compared with control cells (Fig. 5*a*, upper panel). These clones were injected subcutaneously into nude mice and the tumor size was monitored. Strikingly, the tumors formed in mice injected with control LOVO cells grew rapidly, whereas tumors were greatly reduced in mice injected with shRNA stably expressed clones (Figs. 5*a* and 5*b*). These results indicate that eIF4H isoform 1 contributes to the development of colon tumors.

Suppression of eIF4H isoform 1 showed no effect on the growth of immortalized human fibroblasts

The above results have raised the question of whether the decrease of the cell number by eIF4H isoform 1 knockdown is specific to cancer cells or is a more general feature; if it is unique to cancer cells it might be a potential target for cancer therapy. To address this question, we examined the effect of eIF4H suppression on the proliferation of immortalized human fibroblast cell MRC5 using the same siRNA shown in Figure 3. The expression of eIF4H isoforms, especially isoform 1, was greatly suppressed 48 hr after siRNA transfection (Fig. 5*c*). In great contrast with colon cancer cells, there was

ID: jaishankarn | Black Lining: [ON] | Time: 13:39 | Path: N:/3b2/IJC#/Vol00000/100296/APPFile/C2IJC#100296

J_ID: Z3Q Wiley Ed. Ref. No.: 09-2572.R2 Customer A_ID: IJC25419 Date: 12-May-10 Stage: Page: 7

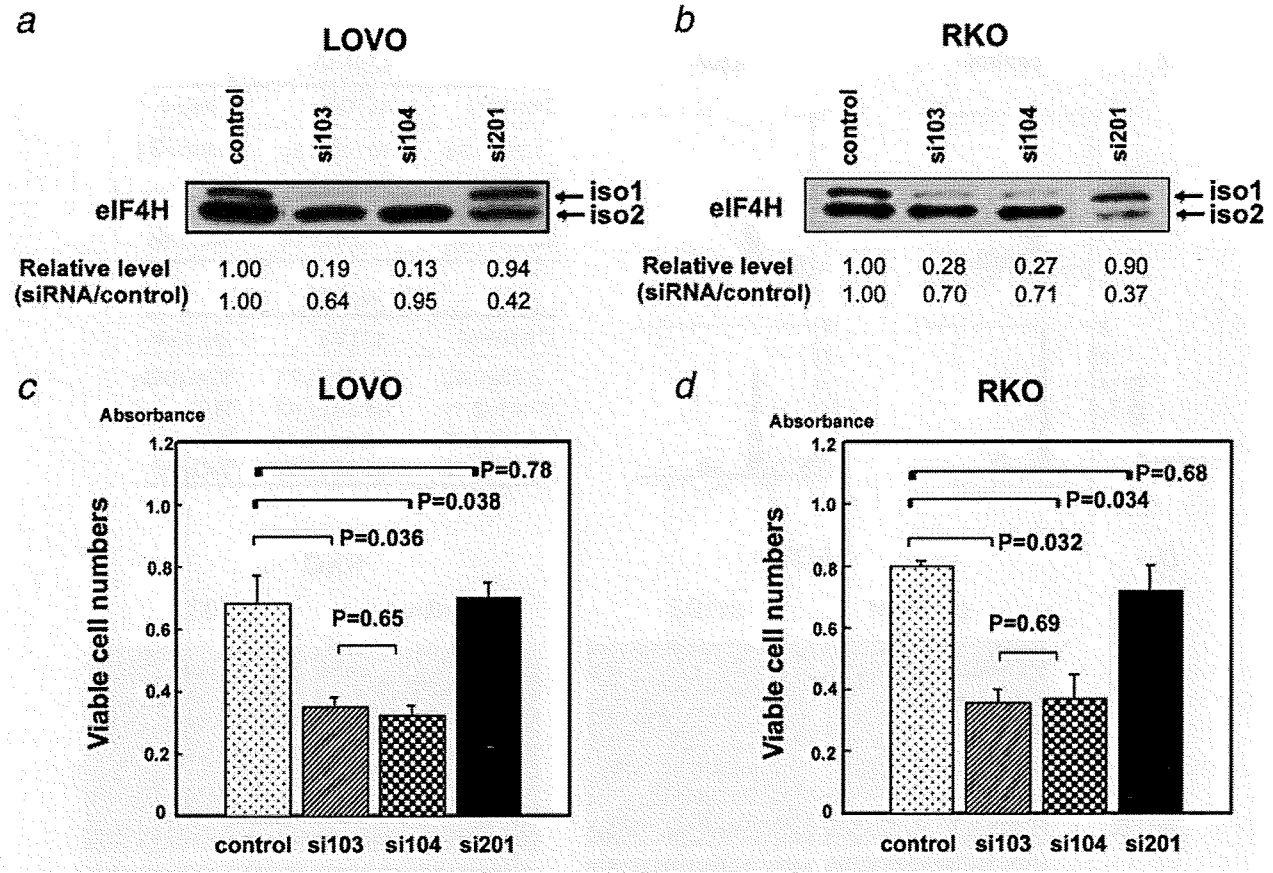

Figure 3. Suppression of eIF4H isoform 1, and not isoform 2, inhibited the growth of colon cancer cell lines. (*a*, *b*) 20 pmol of siRNA (isoform 1 specific: si103, 104; isoform 2 specific: 201) for eIF4H were transfected into LOVO and RKO cells, and the expression of eIF4H isoforms was examined by Western blotting 48 hr after siRNA treatment. The intensity of each band was measured with NIH Image and the relative level of eIF4H isoforms between control and siRNA-treated cells normalized with β-actin was calculated. (*c*, *d*) Viable cell numbers 48 hr after eIF4H siRNA treatment were assessed by MTS assay. Data represent the mean ± SD of eight independent experiments and statistical analysis was performed by Student's *t*-test.

no effect of RNAi on the cell growth of MRC5 (Fig. 5*d*). A similar result was observed in WI38 immortalized lung fibroblast cells (data not shown). Thus, eIF4H isoform 1 might be a suitable therapeutic target for colon cancer.

Possible mechanism of cellular transformation caused by eIF4H isoform 1

What is the mechanism of transformation induced by eIF4H isoform 1 expression? One possible mechanism is that eIF4H isoform 1 leads to the overproduction of potentially oncogenic proteins that stimulate cell proliferation or inhibit apoptosis, such as c-Myc, cyclin D1, VEGF, ODC, Bcl-2 and Bcl-X_L. mRNA of the genes are known to have long and structurally complex 5′-untranslated regions and may require high levels of eIFs, including eIF4H, for their translation. To examine the effect of eIF4H isoform 1 overexpression on the expression of oncogenic proteins, immunoblotting was performed using extracts from NIH3T3 cell lines overexpressing eIF4H isoform 1. Surprisingly, the level of cyclin D1 greatly increased in eIF4H isoform 1-overexpressing cells compared with control cell lines, whereas ODC, Bcl-2 and Bcl-X_L showed only a marginal effect (Figs. 6*a* and 6*b*, Supporting Information Figure 2). Next, we tested whether the suppression of eIF4H isoform 1 decreases the cyclin D1 level. As expected, eIF4H isoform 1-suppressed LOVO cells, sh103-1 and sh103-2, showed marked reduction of cyclin D1 expression (Figs. 6*c* and 6*d*). c-Myc level increased in only one of the eIF4H isoform 1 overexpressing clones and did not decrease in eIF4H stable knockdown cells, which indicates that eIF4H overexpression is not involved in the regulation of c-Myc expression. These results indicate that upregulation of cyclin D1 is involved in the transforming activity of eIF4H isoform 1.

If cyclin D1 upregulation is a direct mechanism of the transforming activity of eIF4H, ectopic expression of cyclin D1 in eIF4H knockdown cells would suppress the inhibitory effect on cell proliferation. To test this, we cotransfected eIF4H isoform 1 siRNA (si104) and cyclin D1 expression

ID: jaishankarn | Black Lining: [ON] | Time: 13:39 | Path: N:/3b2/IJC#/Vol00000/100296/APPFile/C2IJC#100296

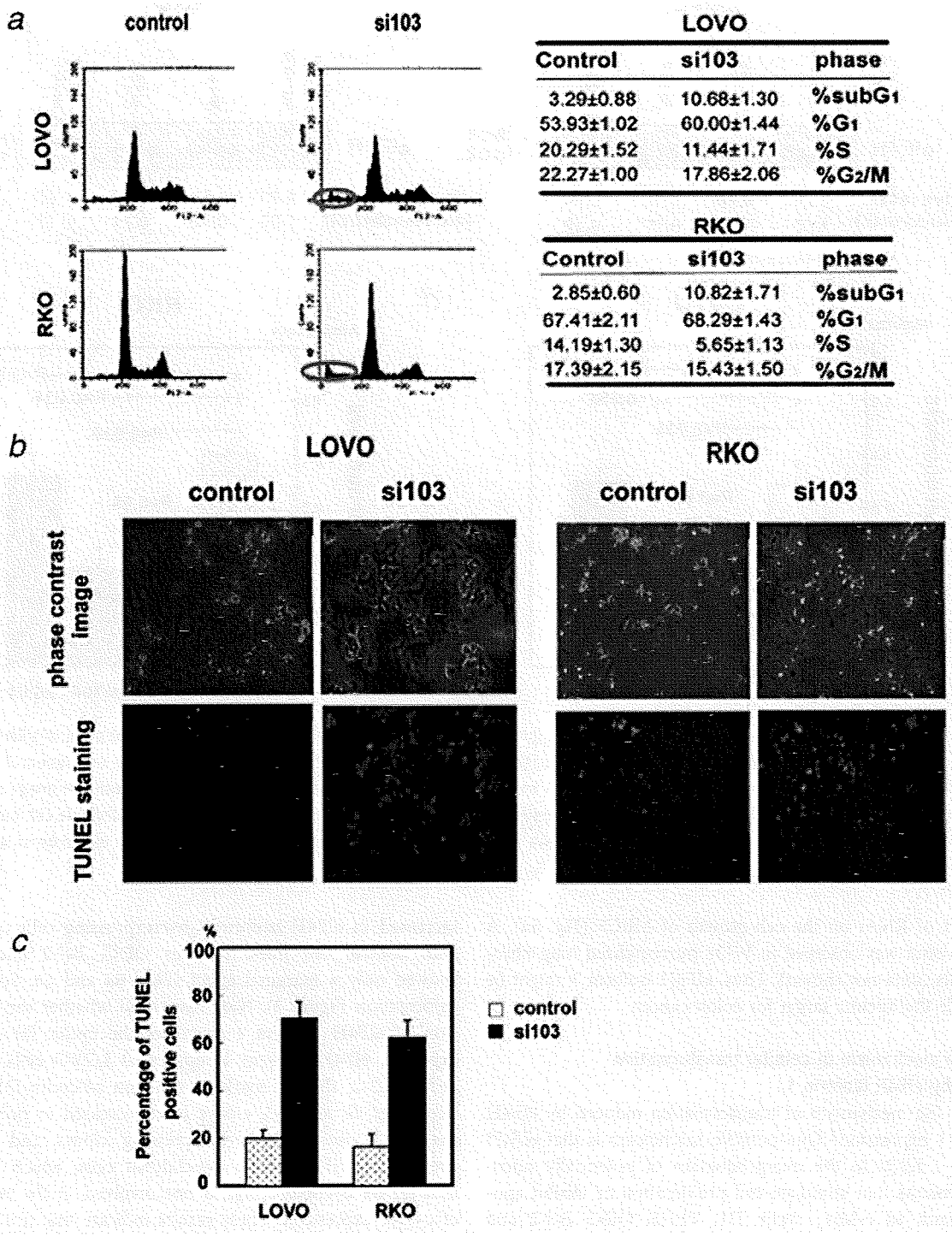

LOVO

Control	si103	phase
3.29±0.88	10.68±1.30	%subG1
53.93±1.02	60.00±1.44	%G1
20.29±1.52	11.44±1.71	%S
22.27±1.00	17.86±2.06	%G2/M

RKO

Control	si103	phase
2.85±0.60	10.82±1.71	%subG1
67.41±2.11	68.29±1.43	%G1
14.19±1.30	5.65±1.13	%S
17.39±2.15	15.43±1.50	%G2/M

Figure 4. Suppression of eIF4H isoform 1 induces apoptosis of colon cancer cell lines. LOVO and RKO cells were treated with 20 pmol of si103, siRNA specific to eIF4H isoform 1, for 48 hr and FACS (*a*) and TUNEL (*b*) analysis was performed. (*a*) FACS analysis was repeated three times and the percentage (mean ± SD) of the cell population in each phase of the cell cycle is shown in the right table. (*b*) TUNEL analysis of control or si103-treated colon cancer cells (LOVO and RKO) showed apoptotic cells. (*c*) The number of TUNEL-positive cells was counted from five different fields. The percentage (mean ± SD) was calculated.

J_ID: Z3Q Wiley Ed. Ref. No.: 09-2572.R2 Customer A_ID: IJC25419 Date: 12-May-10 Stage: Page: 9

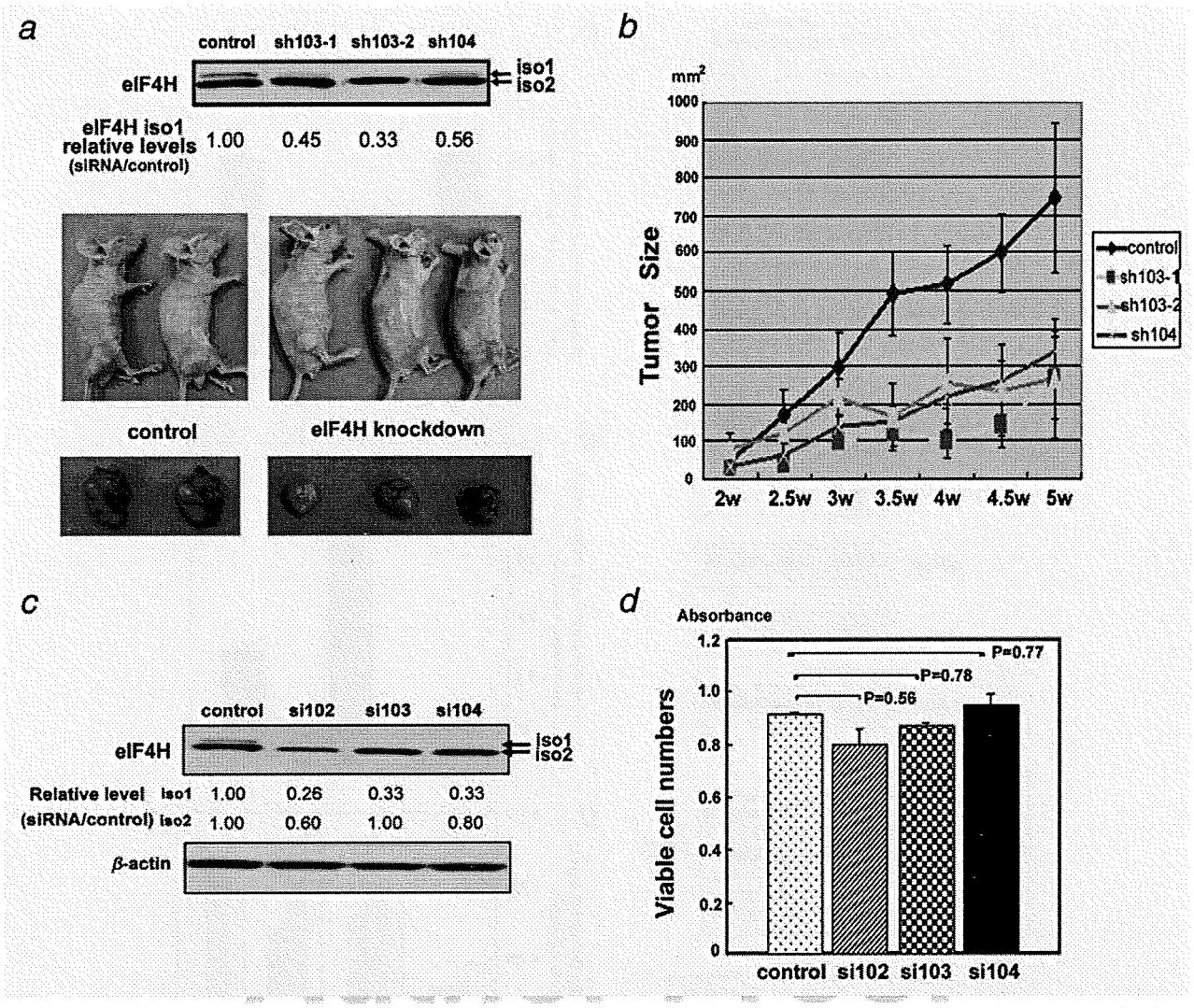

Figure 5. Suppression of eIF4H isoform 1 inhibited tumor growth in nude mice, but showed no effect on the proliferation of immortalized fibroblasts. (*a*) shRNAs (sh103, 104) specific for eIF4H isoform 1 were transfected in LOVO cells and stable knockdown cell lines of eIF4H isoform 1 were generated. sh103-1 and 103-2 are different stable clones generated by sh103 transfection. The suppression of eIF4H isoform 1 in each clone was confirmed by Western blotting. The intensity of each band was measured with NIH image and the relative level of eIF4H isoform 1 between control and stable knockdown cell lines normalized with β-actin was calculated. eIF4H isoform 1 stable knockdown LOVO cells (1×10^6 cells) were subcutaneously injected into nude mice and tumor formation was examined for 5 weeks (lower panel). (*b*) A control and three stable clones, sh103-1, 103-2 and 104, were injected into six mice, respectively. Tumor size was measured every 3 days and tumor growth curves of the mean ± SD of six mice from two independent experiments are shown. (*c*) 20 pmol of siRNA (si102, 103 and 104) for eIF4H were transfected into MRC5 cells and the expression of eIF4H isoforms was examined by Western blotting 48 hr after siRNA treatment. The intensity of each band was measured with NIH image and the relative level of eIF4H isoforms between control and siRNA-treated cells normalized with β-actin was calculated. si102 suppressed both isoform 1 and 2 of eIF4H, whereas si103 and 104 suppressed only isoform 1. (*d*) Viable cell numbers 48 hr after eIF4H siRNA treatment were assessed by MTS assay. Data represent the mean ± SD of eight independent experiments and statistical analysis was performed by Student's *t*-test.

plasmid into a colon cancer cell line, RKO, and measured the viable cell numbers by MTS assay. Expression of the cyclin D1 plasmid was confirmed by Western blotting (Fig. 5*e*). Cotransfection of si104 with control plasmid decreased the cell number, as shown in Figure 3, whereas cotransfection of cyclin D1 expression plasmid reversed the growth suppression effect of si104 (Fig. 5*f*). This result further supports our hypothesis that eIF4H isoform 1 plays an important role in carcinogenesis through the activation of cyclin D1.

The expression of cyclin D1 is well known to be regulated by another eukaryotic translation initiation factor, eIF4E. Regulation is thought to occur at the translational level;

ID: jaishankarn | Black Lining: [ON] | Time: 13:39 | Path: N:/3b2/IJC#/Vol00000/100296/APPFile/C2IJC#100296

COLOR

J_ID: Z3Q Wiley Ed. Ref. No.: 09-2572.R2 Customer A_ID: IJC25419 Date: 12-May-10 Stage: Page: 10

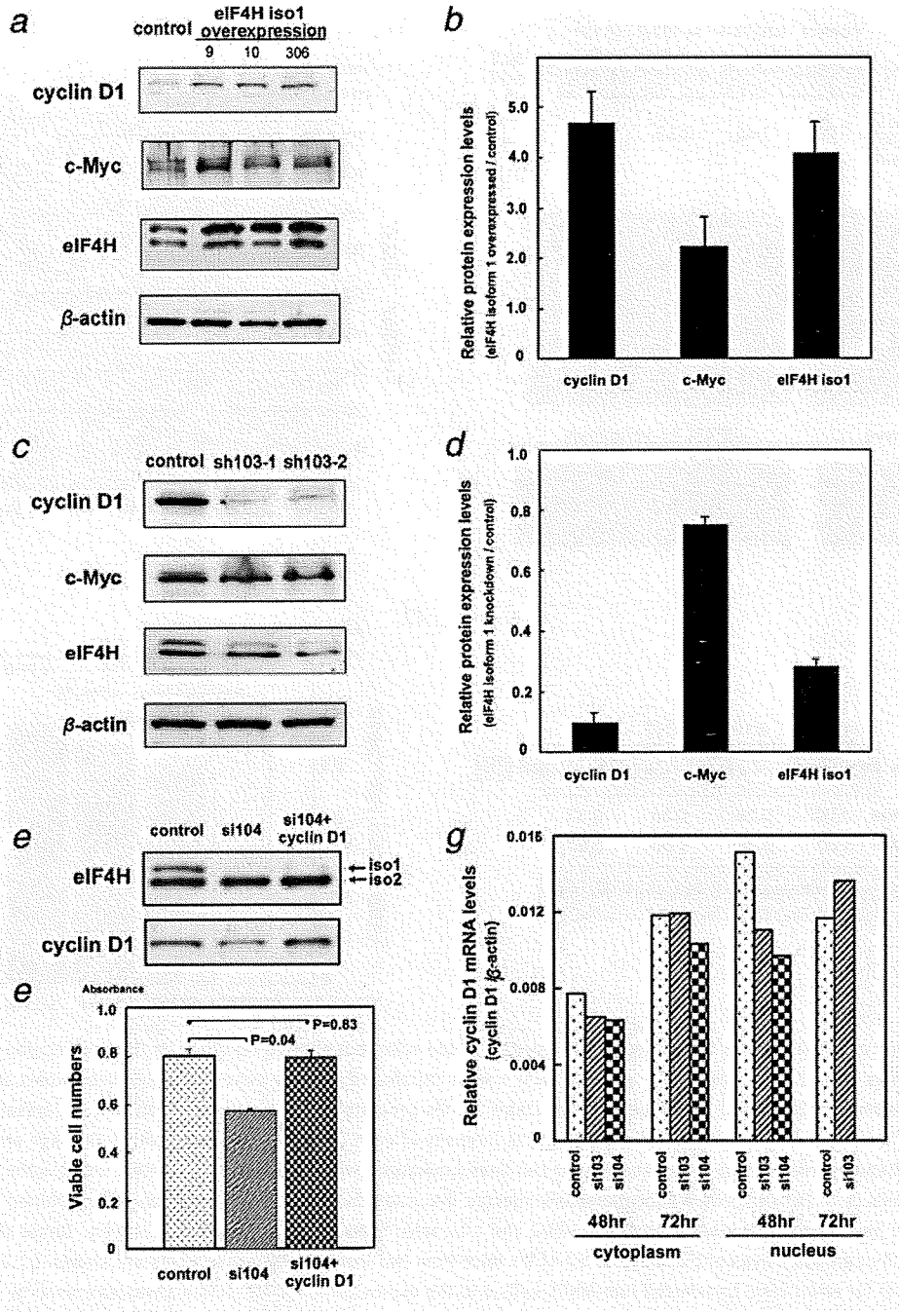

Figure 6. Cyclin D1 upregulation is involved in the transforming activity of eIF4H isoform 1. (*a*) Expressions of cyclin D1 and c-Myc in three different stable clones overexpressing eIF4H isoform 1, no. 9, 10 and 306, were examined with Western blotting. (*b*) The intensity of each band was measured with NIH image and the relative expression levels of each protein normalized with β-actin in eIF4H isoform 1-overexpressing cells compared with control cells are shown. Means and SD values were calculated from the results of the different clones. (*c*) Expression of cyclin D1 and c-Myc was examined in eIF4H isoform 1 stable knockdown LOVO cell lines. (*d*) Data represent the means and SD values calculated from the results of two different clones. (*e*) 50 pmol of eIF4H isoform 1-specific siRNA (si104) with 25 ng of control or cyclin D1 expression plasmid was transfected into RKO cells and the expression of eIF4H isoforms (upper panel) and cyclin D1 (lower panel) was examined by Western blotting 72 hr after siRNA treatment. (*f*) Viable cell numbers 72 hr after transfection were assessed by MTS assay. Data represent the mean ± SD of eight independent experiments and statistical analysis was performed by Student's *t*-test. (*g*) Control or eIF4H isoform 1 siRNA (si103, 104; 50 pmol) was transfected to RKO cells. Total RNA from nucleus and cytoplasm of the cells was extracted 48 and 72 hr after transfection and real-time PCR was performed to examine the cyclin D1 mRNA level. Relative cyclin D1 mRNA levels normalized with β-actin were calculated. Nuclear mRNA level 72 hr after si104 treatment is not shown.

ID: jaishankarn | Black Lining: [ON] | Time: 14:08 | Path: N:/3b2/IJC#/Vol00000/100296/APPFile/C2IJC#100296